Magnetics Information Consortium (MagIC)

Workshop Volume

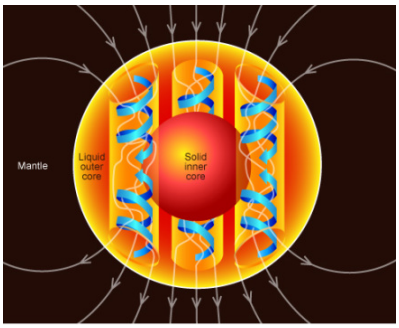

2023 MagIC Workshop

Sponsored by

Welcome to the 2023 MagIC Workshop at the Scripps Institution of Oceanography

Welcome to the shores of the Pacific Ocean for our three-day workshop (Feb 28th - Mar 2nd). We thank you for coming and are looking forward to a successful workshop. First, we have two days of scientific and MagIC data repository related talks. On day three we have group working sessions of how to create contributions, upload them, and download data. We will then show how to and analyze the data using PmagPy and Jupyter notebooks.

We hope you enjoy getting together with members of the paleo, geo, and rock magnetic community and we are glad to have the opportunity to host this meeting.

Anthony Koppers
Nick Jarboe
Rupert Minnett
Nick Swanson-Hysell
Cathy Constable
Lisa Tauxe
Max Brown
Josh Feinberg
Peat Solheid

Table of Contents

Talk Abstracts* - Presentation Order

Poster Abstracts* by First Author

---

* Not all presenters submitted abstracts

Speaker Schedule – Tuesday (Scripps Forum)

8:15	-	9:00	Registration, Poster set-up, and Continental Breakfast
9:00	-	9:05	**Nick Jarboe** - MagIC 2023 Workshop Welcome
9:05	-	9:10	**Raleigh Martin -** A Message from the NSF (recorded)
			Planetary Processes
9:10	-	9:50	**Roger Fu -** Pushing Back the Record of Tectonic Motion and Geodynamo Reversals Using Magnetic Imaging
9:50	-	10:30	**Sonia Tikoo -** Deconvolving the Origin of Lunar Paleomagnetic Records and Implications for an Ancient Dynamo
10:30	-	10:50	Coffee Break and Discussion
10:50	-	11:30	**Dan Thallner** - Coupling Mantle Convection and Geodynamo Simulations to Understand the Influence of Mantle Dynamics on the Generation of Earth's Magnetic Field Throughout the Plate Tectonic Cycle
11:30	-	12:10	**Tinghong Zhou -** Paleomagnetism and the Origin of Inner Core Structure
12:10	-	13:30	Early Career Lunch at the Scripps Forum
			Surface Environments
13:30	-	14:10	**Sarah Slotznick** - Signal Preservation: Global Perspective on Magnetite Dissolution and Local Insights into Greigite Formation
14:10	-	14:50	**France Lagroix** - European Loess and Paleosol Sequences Archiving Quaternary Climate and Environmental Change
14:50	-	15:20	Coffee Break and Discussion
15:20	-	16:00	**Plinio Jaqueto**- Speleothem Formation Processes and Their Impact on Remanence Acquisition
16:00	-	16:40	**Cauê Borlina** - Obtaining High-resolution Paleomagnetic Records from Speleothems using SQUID Microscopy
17:00	-	18:00	Poster Session
18:00	-	20:00	Evening Reception

Speaker Schedule – Wednesday (Scripps Forum)

			MagIC as a Resource for the Community
8:15	-	9:00	Continental Breakfast
9:00	-	9:30	**Anthony Koppers** - MagIC Overview

9:30	-	10:10	**Brendan Cych** - BiCEP and TROUT: Objective Methods for Reanalysis of MagIC Measurement Data
10:10	-	10:30	Coffee Break and Discussion
10:30	-	10:50	**Nick Swanson-Hysell and Rupert Minnett** - Subdomain Views and Breakout Discussion Introduction
10:50	-	11:40	**Breakouts** - (1) Rock magnetism; (2) Paleomagnetic poles; (3) Software tools
11:40	-	12:00	**Breakout Discussion Wrap-up**
12:00	-	13:30	Current Topics Lunch at the Scripps Forum
			Paleogeography
13:30	-	14:10	**Douwe van Hinsbergen** - A New Look on Paleomagnetism in Tectonics: a Global APWP Based on Site-Level Paleomagnetic Data, and the APWP-Online.org Toolbox
14:10	-	14:50	**Mathew Domeier**- Going virtual: constructing APWPs from VGPs
14:50	-	15:20	Coffee Break
15:20	-	16:00	**Stuart Gilder** - An Integrated Magnetic Approach to Solving the Greater India Problem
16:00	-	16:40	**Yiming Zhang** - New perspectives on Laurentia's Grenville Loop: tracking Rodinia across the Mesoproterozoic to Neoproterozoic boundary
16:40	-	16:50	**Nick Jarboe** - Concluding Remarks
16:50	-	17:00	Poster Removal

Group Working and Pop-Up Sessions

Thursday (Ted and Robert Rooms)

9:00	-	10:30	**Introduction to Creating a MagIC Contribution Using Pmag_GUI** - Example work flow of converting from lab format to MagIC format using Pmag_GUI. Make fits to these data using Demag_GUI and then create a file that can be uploaded to MagIC.
10:30	-	10:45	Coffee Break
10:45	-	12:00	**Contributing to MagIC** - Continued tutorial on creating MagIC contributions including discussion of varied data formats and approaches. Bring your own data!
12:00	-	13:00	Working Lunch
13:00	-	14:45	**Interacting with MagIC data using Jupyter notebooks** - Example workflow of downloading data using the MagIC API and interacting with it in notebooks running on JupyterHub.
14:45	-	15:00	Coffee Break
15:00	-	16:50	**Interacting with MagIC data using Jupyter notebooks, Part 2** - Continued examples of plotting and analyzing data from MagIC with time for exploration and questions.
16:50	-	17:00	Wrap-up

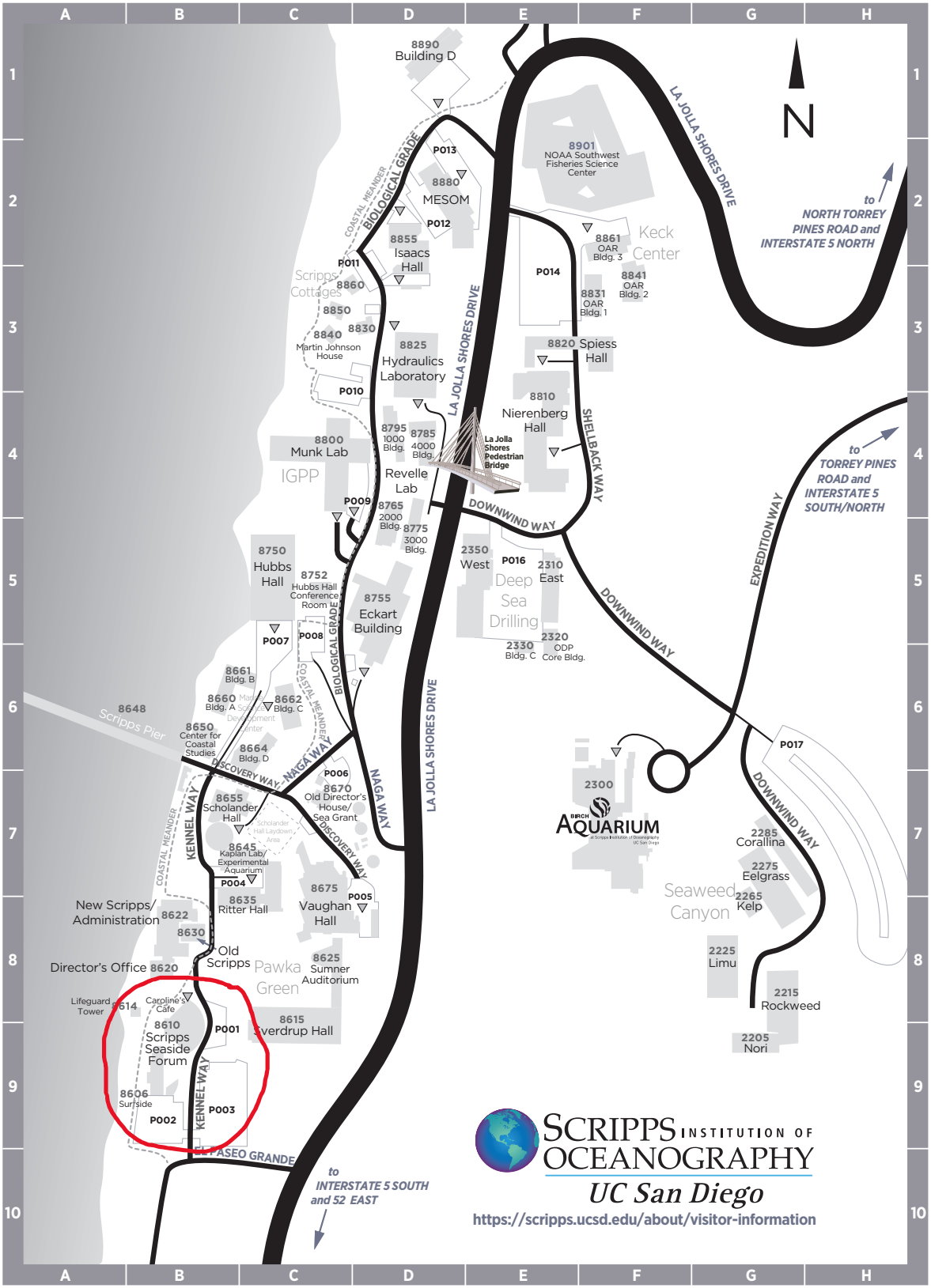

3/2016

Note: Street addresses are listed above the building names. ▽= Service Yard

Attendees

First Name	Last Name	Affiliation	Email
Gary	Acton	Texas A&M University	acton@iodp.tamu.edu
Maggie	Avery	USGS	mavery@usgs.gov
Udo	Barckhausen	BGR	udo.barckhausen@bgr.de
Cauê	Borlina	Johns Hopkins University	csciasc1@jhu.edu
Maxwell	Brown	Institute for Rock Magnetism	mcbrown@umn.edu
Trinity	Carrasco	UCSD, SIO	trinity23carrasco@gmail.com
Nicole	Clizzie	SIO/IGPP	nclizzie@ucsd.edu
Cathy	Constable	UC San Diego	cconstable@ucsd.edu
Steven	Constable	SIO/UCSD	sconstable@ucsd.edu
Brendan	Cych	University of Liverpool	bcych@liverpool.ac.uk
Mathew	Domeier	University of Oslo, Norway	mathewd@geo.uio.no
Kirsten	Elger	GFZ German Research Centre for Geosciences	kelger@gfz-potsdam.de
Joshua	Feinberg	Institute for Rock Magnetism	feinberg@umn.edu
Plinio	Francisco Jaqueto	IRM - UMN	pjaqueto@umn.edu
Roger	Fu	Harvard University	rogerfu12@gmail.com
Anthony	Fuentes	UC Berkeley	anthony.j.fuentes@berkeley.edu
Leandro	Gallo	The Centre for Earth Evolution and Dynamics, Oslo, Norway	l.c.gallo@geo.uio.no
Liang	Gao	China University of Geosciences (Beijing)	lgao@live.cn
Cristina	Garcia-Lasanta	Western Washington University	garcia52@wwu.edu
Natália	Gauer Pasqualon	University of Hawaii at Manoa / Universidade Federal do Rio Grande do Sul	ngp2516@hawaii.edu
Jeff	Gee	Scripps Institution of Oceanography	jsgee@ucsd.edu
Stuart	Gilder	LMU-Munich	gilder@lmu.de
Robert	Hatfield	University of Florida	rhatfield1@ufl.edu
James	Hepworth	University of Plymouth	james.hepworth@plymouth.ac.uk
Vanessa	Israel	Altai Philippines Mining Corporation	vanessaamorisrael@gmail.com
Nicholas	Jarboe	Oregon State	njarboe@earthref.org
Shelby	Jones	New Mexico Office of Archaeological Studies	saj012@ucsd.edu
Ji-In	Jung	Stanford University	jiinjung@stanford.edu
Rachel	Kepler	UCSD, Physics	rkepler@ucsd.edu
Ken	Kodama	Lehigh University	kpk0@lehigh.edu
Anthony	Koppers	Oregon State University	anthony.koppers@oregonstate.edu
France	Lagroix	CNRS - Institut de Physique du Globe de Paris	lagroix@ipgp.fr

Shihu	Li	Institute of Geology and Geology, Chinese Academy of Sciences	lsh917@mail.iggcas.ac.cn
Elias	Mansbach	Massachusetts Institute of Technology	mansbach@mit.edu
Phil	McCausland	University of Western Ontario	pmccausl@uwo.ca
Rupert	Minnett	Oregon State University	rminnett@earthref.org
Matti	Morzfeld	UCSD, IGPP	mmorzfeld@ucsd.edu
Jayaraju	Nadimikeri	Yogi Vemana University	nadimikeri@gmail.com
Leyla	Namazie	University of California, Berkeley	leylanamazie@berkeley.edu
Ellen	Nelson	University of Wisconsin– Madison	emnelson8@wisc.edu
Claire	Nichols	University of Oxford	claire.nichols@earth.ox.ac.uk
Anthony	Pivarunas	U.S. Geological Survey	apivarunas@usgs.gov
Sandra B	Ramirez-Garcia	University of Utah	sand.ramirezgarcia@utah.edu
Brendan	Reilly	Lamont-Doherty Earth Observatory, Columbia University	breilly@ldeo.columbia.edu
Sara	Satolli	University of Chieti-Pescara (Italy)	s.satolli@unich.it
Jairo	Savian	Universidade Federal do Rio Grande do Sul - UFRGS	jairo.savian@ufrgs.br
Gary	Scott	Berkeley Geochronology Center	gscott@bgc.org
Sarvendra	Singh	Birbal Sahni Institute of palaeosciences, Lucknow	chauhansp122@gmail.com
Sarah	Slotznick	Dartmouth College	sslotz@dartmouth.edu
Peter	Solheid	IRM	peat@umn.edu
Nicholas	Swanson-Hysell	UC Berkeley	swanson-hysell@berkeley.edu
John	Tarduno	University of Rochester	john.tarduno@rochester.edu
Lisa	Tauxe	SIO	ltauxe@ucsd.edu
Daniele	Thallner	University of Florida	d.thallner@ufl.edu
Sonia	Tikoo	Stanford University	smtikoo@stanford.edu
Justin	Tonti-Filippini	LMU Munich	j.tonti@lmu.de
Alexander	Tully	University of Liverpool	a.tully@liverpool.ac.uk
Douwe	van Hinsbergen	Utrecht University, the Netherlands	d.j.j.vanhinsbergen@uu.nl
Yi	Xue	University of Oslo	yi.xue@geo.uio.no
Hong	Yang	Stanford University	hyang777@stanford.edu
Yiming	Zhang	UC Berkeley	yimingzhang@berkeley.edu
Tinghong	Zhou	University of Rochester	tzhou16@ur.rochester.edu

Pushing back the record of tectonic motion and geodynamo reversals using magnetic imaging

Roger R. Fu[1], Alec R. Brenner[1], Sarah C. Steele[1]
[1]Department of Earth and Planetary Sciences, Harvard University, Cambridge, MA, USA.

A magnetic core dynamo and mobile lid plate tectonics are two planetary-scale geophysical processes that exert fundamental controls on the surface environment. A dynamo can promote or prevent atmospheric loss to interplanetary space while plate tectonics shape surface chemistry and temperature by governing the input and erosion fluxes of biologically important light elements such as C and P. Due to these effects, describing the onset and cessation of these processes is key to understanding planetary habitability.

We will present the results of studies on the martian meteorite ALH 84001 and 3.18-3.25 Ga terrestrial rocks from the Pilbara Craton. First, we find that 100 μm scale ferromagnetic assemblages in ALH 84001 are magnetized in two sets of directions approximately 140˚ apart (Fig. 1; Steele et al., *in revision*). Rock magnetic characterization of these chromite-sulfide assemblages indicates that they are capable of recording microtesla-level magnetic fields. Meanwhile, mesoscale impact modeling shows that shock events between 10 and 30 GPa can remagnetize 100 μm-scale sub-volumes of ALH 84001 material while only weakly heating neighboring regions.

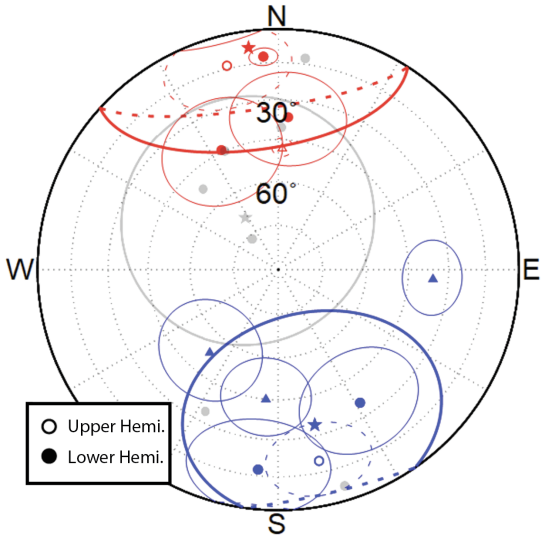

Figure 1: Distribution of magnetizations in ALH 84001. Red and blue data points denote high coercivity (circles) or high temperature (triangles) magnetization component directions from each of two groups of chromite-sulfide assemblages. Gray points correspond to fusion crust directions.

Combining these observations, we conclude that the two magnetization directions record ancient martian magnetic fields during two distinct impact events. Given the history of ALH 84001, these events may have occurred at 4.1, 3.9, or 1.2 Ga, thereby requiring a strong surface magnetic field on Mars at or before 3.9 Ga. Further, our statistical analysis shows a reversing magnetic core dynamo is more likely to explain the large angular separation between the two directions. The persistence of a martian core dynamo until at least 3.9 Ga implies the presence of a global magnetic field during at least the first several hundred My of valley network formation on Mars. This magnetic field likely played an active role in controlling atmospheric composition during this hydrologically active portion of martian history,

although its exact effect on atmospheric loss remains to be quantified.

Second, our paleomagnetic analyses of metavolcanic rocks from the 3.18 Ga Honeyeater basalts and 3.25 Ga Kunagunarrina Formation show that the Pilbara Craton underwent translation and rotation at rates greater than 0.55° per My during the 3.34-3.18 Ga interval (Brenner et al. 2020, 2022). The Euler pole positions for these motions are difficult to reconcile with true polar wander while the high minimum velocity is likely inconsistent with single-plate, net lithosphere rotation. We therefore conclude that mobile-lid plate tectonics, with its implications for global temperature regulation and light element cycling, were likely established on Earth by 3.25 Ga, which is earlier than inferred from some recent geochemical studies. Finally, Kunagunarrina Formation rocks record a geomagnetic reversal at 3.25 Ga, implying a relatively dipolar, core-generated geodynamo with implications for Earth's atmospheric loss history and the validity of Archean paleomagnetism.

Micrometer-scale magnetic field imaging played a critical role in both sets of studies described above. The high spatial resolution of the quantum diamond microscope (QDM) enabled net magnetic moment recovery from individual chromite-sulfide assemblages in ALH 84001 for the first time. Meanwhile, identification of the ferromagnetic sources with specific alteration mineral assemblages in the Honeyeater basalt and Kunagunarrina Formation metavolcanics shows with high confidence that the magnetization is a thermochemical remanent magnetization (TCRM) acquired during seafloor alteration. This observation then allowed direct dating of the magnetization using the associated secondary phases. These results therefore demonstrate the potential of the QDM for expanding the set of magnetic materials amenable to paleomagnetic analysis and for strengthening the interpretation of traditional samples by revealing the mineralogical basis of magnetization.

References

S. Steele, R.R. Fu, M.W.R. Volk, T.L. North, A.R. Brenner, G.S. Collins, T.M. Davison, A.R. Muxworthy. (*in revision*) Paleomagnetic evidence for a long-lived potentially reversing martian dynamo at ~3.9 Ga. *Sci. Adv.*

A.C. Brenner, R.R. Fu**,** D.A.D. Evans, A.V. Smirnov, R. Trubko, I. Rose (2020) Paleomagnetic evidence for modern-like plate motion velocities at 3.2 Ga. *Sci. Adv.* 6, eaaz8670.

A.R. Brenner, R.R. Fu, A.R.C. Kylander-Clark, G.J. Hudak, B.J. Foley. (2022) A record of plate motion and a geomagnetic reversal at 3.25 Ga. *PNAS* 119, e2210258119.

Deconvolving the Origin of Lunar Paleomagnetic Records and Implications for an Ancient Dynamo

S. M. Tikoo, J. Jung
Department of Geophysics, Stanford University, Stanford, CA 94305

Orbital measurements of lunar crustal fields as well as paleomagnetic measurements of Apollo and Chang'e-5 samples collectively indicate that lunar rocks contain natural remanent magnetization (NRM). Paleointensities of ~1-100 μT have been obtained from returned lunar samples aged between 4.25 ± 0.01 and 1.47 ± 0.45 Ga [*Cai et al.*, 2022; *Wieczorek et al.*, in press]. Assuming that these magnetic records were acquired on the Moon, the most likely field sources are an ancient dynamo field and impact-generated fields. Dynamo fields are expected to be temporally stable over the primary cooling periods of rock samples, while transient impact-related fields may persist from <1s (for the smallest impacts) up to ~1 day (for large basin-forming impacts) [*Crawford*, 2020; *Crawford and Schultz*, 1999; *Hood and Artemieva*, 2008].

Most modern paleomagnetic studies have analyzed mare basalts. These mare basalts display no petrographic evidence of shock, indicating peak pressures <5 GPa. $^{40}Ar/^{39}Ar$ thermochronology studies on several of these samples indicate that they have largely undisturbed thermal histories after their formation. The slow (>1 h) cooling timescales of these basalts preclude acquisition of thermoremanent magnetization (TRM) from impact fields as the origin of remanence. Impacts may be capable of imparting rocks with shock remanent magnetization (SRM) [*Gattacceca et al.*, 2010], but pressure experiments on mare basalts have demonstrated that pressure remanent magnetization (PRM, an SRM analog) is preferentially removed via alternating field (AF) demagnetization <50 mT. In contrast, the NRM in some mare basalts persists to higher AF levels. Given the above considerations, the paleomagnetic records of mare basalts aged 3.85-3.56 Ga have been interpreted as evidence for a lunar dynamo by several studies [*Cournède et al.*, 2012; *Nichols et al.*, 2021; *Shea et al.*, 2012; *Suavet et al.*, 2013]. Following this interpretation, the lunar dynamo would have operated at least intermittently beyond 3.56 Ga until its cessation sometime before 1 Ga [*Mighani et al.*, 2020].

Until recently, all modern paleomagnetic studies of lunar samples <1 Ga found no evidence of magnetizing fields [*Buz et al.*, 2015; *Mighani et al.*, 2020; *Tikoo et al.*, 2017]. However, a recent paleomagnetic study of the 2 Ma impact melt sample 64455,24 retrieved a high paleointensity (10-89 μT) [*Tarduno et al.*, 2021]. Due to its young age, such a high paleointensity would necessitate magnetization from a non-dynamo field. The same study also observed that several fragments taken from mare basalts with ages spanning ~3.9-3.2 Ga appeared to be unmagnetized. As a result, *Tarduno et al.* [2021] posited that impact-related fields magnetized lunar crustal rocks rather than a long-lived dynamo field. Other works have posited that lunar paleomagnetic records may instead reflect magnetic contamination acquired from exposure to 3-5 mT fields on the Apollo return spacecraft [*Lawrence et al.*, 2008]. In this presentation, we review the modern lunar paleomagnetic record and discuss the evidence for and against a long-lived lunar dynamo. Then we present results from new studies that are aimed at deciphering the origin of lunar paleomagnetic records.

First, we explore whether lunar paleomagnetic records could be the result of magnetic contamination from spacecraft fields. In a series of controlled experiments, we subjected several lunar rocks to fields of 5-10 mT for varying durations with the goal of assessing how easily the resulting isothermal and viscous remanences (IRM and VRM, respectively) could be cleaned using stepwise AF demagnetization. We found that AF demagnetization was largely successful at removing these remanences from mare basalts and that reliable paleointensities can be obtained

from utilizing demagnetization data at higher (>50 mT) AF levels using the ARM paleointensity method. Therefore, we conclude that the high coercivity remanent magnetizations observed within several mare basalts were acquired on the Moon and do not represent magnetic contamination acquired during or after the Apollo missions. Impact melt-bearing lithologies are more susceptible to viscous contamination that may not be as easily removed using AF demagnetization methods. To mitigate this, we suggest studying lunar impactite samples using a combination of AF and thermal demagnetization to ensure robustness of paleomagnetic results.

Next, we present results from a new paleomagnetic study of four ~3.9-3.5 Ga Apollo 11 mare basalt samples: 10003, 10044, 10069, and 10071. Intriguingly, sample 10044 exhibits petrographic evidence of shock (peak pressure ~12 GPa) and does not contain stable high coercivity remanence. The paleomagnetic record of this sample could reflect shock demagnetization in a weak to null field rather than SRM from an impact field. In contrast, the high coercivity magnetization components within the unshocked (<5 GPa) samples 10069 and 10071 yielded paleointensities of ~25 μT and ~5 μT, respectively. If these rocks contain dynamo records, this paleointensity variability may reflect secular changes in field behavior. Ongoing work aims to distinguish between the dynamo and impact field hypotheses for the NRM in these samples.

References:

Buz, J., B. P. Weiss, S. M. Tikoo, D. L. Shuster, J. Gattacceca, and T. L. Grove (2015), Magnetism of a very young lunar glass, *J. Geophys. Res.*, *120*, doi:10.1002/2015JE004878.

Cai, S., H. Qin, C. Deng, S. Liu, Y. Chen, H. He, and Y. Pan (2022), Magnetic properties and paleointensity of lunar soil sample (E21), *Acta Petrol. Sin.*, *38*(6), 1832-1842.

Cournède, C., J. Gattacceca, and P. Rochette (2012), Magnetic study of large Apollo samples: Possible evidence for an ancient centered dipolar field on the Moon, *Earth Planet. Sci. Lett.*, *331-332*, 31-42.

Crawford, D. A. (2020), Simulations of magnetic fields produced by asteroid impact: Possible implications for planetary paleomagnetism, *Int. J. Impact Eng.*, *137*, 103464, doi:10.1016/j.ijimpeng.2019.103464.

Crawford, D. A., and P. H. Schultz (1999), Electromagnetic properties of impact-generated plasma, vapor and debris, *Int. J. Impact Eng.*, *23*, 169-180.

Gattacceca, J., M. Boustie, L. L. Hood, J.-P. Cuq-Lelandais, M. Fuller, N. S. Bezaeva, T. de Resseguier, and L. Berthe (2010), Can the lunar crust be magnetized by shock: Experimental groundtruth, *Earth Planet. Sci. Lett.*, *299*, 42-53.

Hood, L. L., and N. A. Artemieva (2008), Antipodal effects of lunar basin-forming impacts: Initial 3D simulations and comparisons with observations, *Icarus*, *193*, 485-502.

Lawrence, K., C. Johnson, L. Tauxe, and J. S. Gee (2008), Lunar paleointensity measurements: Implications for lunar magnetic evolution, *Phys. Earth Planet. Inter.*, *168*, 71-87.

Mighani, S., H. Wang, D. L. Shuster, C. S. Borlina, C. I. O. Nichols, and B. P. Weiss (2020), The end of the lunar dynamo, *Sci. Adv.*, *6*(eaax0883), 1-8.

Nichols, C. I. O., B. Weiss, B. Getzin, H. Schmitt, A. Beguin, A. Rae, and J. Shah (2021), The paleoinclination of the ancient lunar magnetic field from an Apollo 17 basalt, *Nat. Astron.*, *5*, 1216-1223.

Shea, E. K., B. P. Weiss, W. S. Cassata, D. L. Shuster, S. M. Tikoo, J. Gattacceca, T. L. Grove, and M. D. Fuller (2012), A long-lived lunar core dynamo, *Science*, *335*, 453-456.

Suavet, C., B. P. Weiss, W. S. Cassata, D. L. Shuster, J. Gattacceca, L. Chan, I. Garrick-Bethell, J. W. Head, T. L. Grove, and M. D. Fuller (2013), Persistence and origin of the lunar core dynamo, *Proc. Natl. Acad. Sci. USA*, *110*(21), 8453-8458, doi:10.1073/pnas.1300341110.

Tarduno, J. A., et al. (2021), Absence of a long-lived lunar paleomagnetosphere, *Sci. Adv.*, *7*, eabi7647, doi:10.1126/sciadv.abi7647.

Tikoo, S. M., B. P. Weiss, D. L. Shuster, C. Suavet, H. Wang, and T. L. Grove (2017), A two-billion-year history for the lunar dynamo, *Sci. Adv.*, *3*(8), e1700207, doi:10.1126/sciadv.1700207.

Wieczorek, M. A., et al. (in press), Lunar magnetism, in *New Views of the Moon II, Rev. Mineral. Geochem.*, edited.

Paleomagnetism and the origin of inner core structure

Tinghong Zhou[1], John A. Tarduno[1,2,3], Francis Nimmo[4], Rory D. Cottrell[1], Richard K. Bono[5,6], Mauricio Ibanez-Mejia[7], Wentao Huang[8], Matt Hamilton[9], Kenneth Kodama[10], Aleksey V. Smirnov[11,12]

[1] Department of Earth & Environmental Sciences, University of Rochester, Rochester, NY, 14627 USA.
[2] Department Physics and Astronomy, University of Rochester, Rochester, NY 14627, USA.
[3] Laboratory for Laser Energetics, University of Rochester, Rochester, NY 14623, USA.
[4] Department Earth and Planetary Sciences, University of California, Santa Cruz, CA 95064, USA.
[5] Department Earth, Ocean and Atmospheric Science, Florida State University, Tallahassee, FL 32306, USA.
[6] Geomagnetism Laboratory, University of Liverpool, Liverpool L69 3GP, UK.
[7] Department Geosciences, University of Arizona, Tucson, AZ 85721, USA.
[8] Institute of Tibetan Plateau Research, Chinese Academy of Sciences, Beijing, China.
[9] School of Geosciences, University of Oklahoma, Norman, OK, USA.
[10] Department of Earth and Environmental Sciences, Lehigh University, Bethlehem, PA 18015, USA.
[11] Department of Geological Mining Engineering and Sciences, Michigan Technological University, Houghton, MI 49931, USA.
[12] Department of Physics, Michigan Technological University, Houghton, MI 49931, USA.

Present-day variations in the rate of growth of the inner core have been related to heterogeneity of heat loss at the core-mantle boundary (Aubert et al., 2008). The present-day structure of the deep mantle is dominated by a spherical harmonic degree-2 pattern. A change in seismic anisotropy, defining an innermost and outermost inner core, occurs at ~650 km radius (Stephenson et al., 2021). This change could indicate that a relict of an older degree-1 pattern of deep mantle structure has been preserved in the structure of the inner core. But heretofore, the age of this potential change, which in turn could relate to the long-term surface plate tectonic regime, has been unconstrained.

Ascertaining the inner core nucleation age is a key to understanding the origin of the change in inner core structure. Using single crystal paleointensity (SCP) analyses (Tarduno et al., 2006) with CO_2 laser heating, Bono et al. (2019) discovered a time-averaged ultra-low field from ~565 Ma Sept-Îles intrusive suite anorthosites. The silicate crystals analyzed had rock magnetic and electron microscope characteristics that demonstrated the dominance of single domain magnetic recorders. The paleofield strength was lower than 10% of the geomagnetic field strength today, and time-averaged because of the relatively slow cooling of the Sept-Îles intrusive suite. Together with results from a host of studies indicating an unusual field, Bono et al. (2019) proposed the Ediacaran time-averaged ultra-low field to be a fingerprint of inner core nucleation. The ultra-low field state is consistent with some geodynamo simulations that predict that prior to inner core nucleation, the core's kinetic energy should approach or exceed the magnetic energy, leading to a collapse of magnetic field (Driscoll, 2016). The Ediacaran age matches well with the predicted inner core nucleation time from thermal models (e.g., around 500 Ma predicted by Nimmo, 2015).

The Ediacaran ultra-low field was later supported by other paleointensity studies from the East European Craton (Shcherbakova et al., 2020) and Grenville dikes of Canada (Thallner et al., 2021). Low geomagnetic field values have also been reported from other ages, such as from the Devonian (~ 400 Ma dykes from the Southern Urals (Shcherbakova et al., 2021)). However, these appear to define geomagnetic behavior different from that of the Ediacaran Period in that higher values are also observed. There are also continued concerns over data reliability both because of multidomain effects in the whole rocks sampled and the potential for low-field bias, and/or potential unremoved overprints/remagnetizations. Currently, the Ediacaran Period ultra-low field is notable in having data from global-dispersed locations, and independent thermal and geodynamo models predicting this as the time of inner core nucleation (Nimmo, 2015; Driscoll, 2016; Davies et al., 2022).

Inner core nucleation provides new energy sources, such as the latent heat released during Fe solidification and buoyancy caused by expulsed light elements, to power the dynamo. With such additional energy sources, the geomagnetic field strength should increase. However, it has been unclear how long the

Ediacaran ultra-low field state lasted, and how the field recovered. In this study, we investigated the paleointensity recorded by the ~532 Ma Glen Mountains Layered Complex (GMLC) anorthosite using SCP analyses. Plagioclase crystals clean of other minerals (e.g., pyroxene) ~3 mm in size were picked from rock crushes of the anorthosite. Importantly, magnetic hysteresis loops and first order reversal curves show a dominance of single domain magnetic behavior, separating these magnetic recorders from whole rocks which contain multidomain components. Data from scanning electron microscopy further documents that elongated single domain titanomagnetite and magnetite needles are the dominant magnetic carriers in these plagioclase crystals. We performed Thellier-Coe measurements on the crystals accompanied with partial thermal remanence (pTRM) checks. Seventeen samples passed our paleointensity selection criteria. The cooling time of the GMLC anorthosite is about 500 kyr (Wall et al., 2021), sufficient to average geomagnetic field secular variation. We also considered potential applied magnetic field dependence on the paleointensity results; the data show no significant dependence. After cooling rate and anisotropy corrections, the averaged paleointensity we acquired is 13.7 ± 3.4 μT, and the corresponding paleomagnetic dipole moment (PDM) is $3.5 \pm 0.9 \times 10^{22}$ A m^2.

Our high quality, time-averaged PDM results from ~532 Ma GMLC anorthosite plagioclase crystals are about 5 times higher than the Ediacaran ultra-low field intensity (~ 0.7×10^{22} A m^2, Bono et al., 2019). This indicates a rapid recovery of the geomagnetic field strength, within ~33 Myr. Such a rapid increase is consistent with the prediction that the nucleation of the inner core adds new energy sources to the dynamo; therefore, our results in turn further support an Ediacaran inner core nucleation age. Our new PDM (Zhou et al., 2022) along with the PDM reported by Bono et al. (2019) provide a constraint for the inner core nucleation onset time of ~550 Ma. A thermal evolution model (Nimmo, 2015) using this onset age shows that the inner core grew to half its current radius, where the boundary between the innermost and outermost inner core is located, at ~450 Ma. Therefore, we suggest the present deep mantle degree-2 structure recorded by the outermost inner core formed after ~ 450 Ma, while the prior degree-1 structure is preserved in the structure of the innermost inner core (Zhou et al., 2022).

References:

Aubert, J., Amit, H., Hulot, G., & Olson, P. (2008). Thermochemical flows couple the Earth's inner core growth to mantle heterogeneity. *Nature*, *454*(7205), 758-761.

Bono, R. K., Tarduno, J. A., Nimmo, F., & Cottrell, R. D. (2019). Young inner core inferred from Ediacaran ultra-low geomagnetic field intensity. *Nature Geoscience*, *12*(2), 143-147.

Davies, C. J., Bono, R. K., Meduri, D. G., Aubert, J., Greenwood, S., & Biggin, A. J. (2022). Dynamo constraints on the long-term evolution of Earth's magnetic field strength. *Geophysical Journal International*, *228*(1), 316-336.

Driscoll, P. E. (2016). Simulating 2 Ga of geodynamo history. *Geophysical Research Letters*, *43*(11), 5680-5687.

Nimmo, F., & Schubert, G. (2015). Thermal and compositional evolution of the core. *Core Dynamics, Treatise on Geophysics*, 217-241.

Shcherbakova, V. V., Zhidkov, G. V., Shcherbakov, V. P., Golovanova, I. V., Danukalov, K. N., & Salmanova, R. Y. (2021). Ultra-low geomagnetic field intensity in the Devonian obtained from the Southern Ural Rock Studies. *Izvestiya, Physics of the Solid Earth*, *57*, 900-912.

Shcherbakova, V. V., Bakhmutov, V. G., Thallner, D., Shcherbakov, V. P., Zhidkov, G. V., & Biggin, A. J. (2020). Ultra-low palaeointensities from East European Craton, Ukraine support a globally anomalous palaeomagnetic field in the Ediacaran. *Geophysical Journal International*, *220*(3), 1928-1946.

Stephenson, J., Tkalčić, H., & Sambridge, M. (2021). Evidence for the innermost inner core: Robust parameter search for radially varying anisotropy using the neighborhood algorithm. *Journal of Geophysical Research: Solid Earth*, *126*(1), e2020JB020545.

Tarduno, J. A., Cottrell, R. D., & Smirnov, A. V. (2006). The paleomagnetism of single silicate crystals: Recording geomagnetic field strength during mixed polarity intervals, superchrons, and inner core growth. *Reviews of Geophysics*, *44*(1).

Thallner, D., Biggin, A. J., & Halls, H. C. (2021). An extended period of extremely weak geomagnetic field suggested by palaeointensities from the Ediacaran Grenville dykes (SE Canada). *Earth and Planetary Science Letters*, *568*, 117025.

Wall, C. J., Hanson, R. E., Schmitz, M., Price, J. D., Donovan, R. N., Boro, J. R., ... & Toews, C. E. (2021). Integrating zircon trace-element geochemistry and high-precision U-Pb zircon geochronology to resolve the timing and petrogenesis of the late Ediacaran–Cambrian Wichita igneous province, Southern Oklahoma Aulacogen, USA. *Geology*, *49*(3), 268-272.

Zhou, T., Tarduno, J. A., Nimmo, F., Cottrell, R. D., Bono, R. K., Ibanez-Mejia, M., ... & Padgett III, F. (2022). Early Cambrian renewal of the geodynamo and the origin of inner core structure. *Nature communications*, *13*(1), 4161.

Signal Preservation: Global Perspective on Magnetite Dissolution and Local Insights into Greigite Formation

Sarah P. Slotznick[1*], Jack Kreisler[1], Josephine G. Benson[1], Roger R. Fu[2], William D. Leavitt[1]

[1] Dartmouth College, Hanover, NH 03755 USA
[2] Harvard University, Camrbridge, MA 02138 USA
*sslotz@dartmouth.edu

Much of paleomagnetism critically depends on the preservation of detrital magnetic grains in sediments and sedimentary rocks. However, diagenesis is a process that, by definition, has occurred in all sedimentary rocks and often has begun in sediments; during this process, detrital grains are dissolved and new minerals form. Here we will present two studies on these processes in the modern, which highlight potential new directions for the MagIC database. While it is qualitatively understood from magnetic analyses that diagenetic dissolution of magnetite is common in marine sediments, there is no general model for magnetite preservation. We analyzed previously published rock magnetic data from nineteen marine sediment cores across the globe and calculated absolute magnetite abundance. These abundance data were compared to factors such as total organic carbon (TOC), pore water sulfate, and sedimentation rate to see how they affected magnetite diagenesis. Sulfate has the most direct influence on magnetite diagenesis, while TOC has the least direct influence. It is difficult to disentangle site-specific from general diagenetic factors, so a quantitative model of magnetite preservation remains out of reach. However, magnetite abundances tend to fall between 100 and 500 ppm, which provide a frame of reference for deep-time environmental magnetism.

On a more local scale, we probed greigite formation in four euxinic (anoxic and sulfidic) meromictic lakes in New Hampshire to provide an expanded window into pore-water processes that can occur on the centimeter-scale. We applied bulk hysteresis, direct current demagnetization curves with magnetic unmixing, and first-order reversal curves on filtered water column and sediment samples. Magnetic mineralogy and grainsize is complex in these samples changing by depth, season, and site, but using the gyroremanent magnetic property of greigite, we were able to confidently identify greigite in some, but not all, of the sediments. Our ongoing research highlights the important role of environmental chemistry in greigite formation and has implications for assessing the potential for this diagenetic phase in sedimentary archives. These types of modern environmental magnetic analyses directly connect to paleomagnetism and provide new pathways for interpreting the magnetic directions recorded in ancient sedimentary rocks.

European loess and paleosol sequences archiving Quaternary climate and environmental change

France Lagroix

CNRS - Institut de Physique du Globe de Paris

Loess and paleosol sequences are remarkable archives of continental paleoclimate. It is known since the 1980's that magnetic susceptibility variations between loess and intercalated soils track glacial and interglacial cycles, illustrating the loess magnetism - climate connection. The European Loess Belt results from a complex interplay of processes producing a supply of mineral dust, atmospheric circulation that can readily uplift and transport the mineral dust and continental surfaces that geomorphologically are prone to trapping and accumulating deposited airborne mineral dust. Thereafter, the alteration undergone by the accumulated loess depends on prevailing climate conditions. Loess and paleosol sequence across the European Loess Belt record climate change on glacial to interglacial timescale and also on shorter timescales. The presentation aims to demonstrate that mineral magnetism is one analytical approach, among others, providing insightful data useful for the reconstruction of Quaternary climate and environmental change across continental Europe.

Speleothem formation processes and their impact on remanence acquisition

Plinio Francisco Jaqueto

Institute of Rock Magnetism, University of Minnesota

The development of paleoenvironmental information using speleothems since the 90's, provided valuable terrestrial records to our understanding of climate change at different timescales. The development of U-Th dating, associated with oxygen and carbon isotopes, cave monitoring, monsoon history, multiproxy at submillimeter scale allow these records to be annually resolved and boosts the understanding of forecasting by providing data that can be compared to general circulation models. Since 2010, speleothem magnetism has been revisited and more studies are now available. The significance of the magnetic minerals in these records were tested in climate extremes (such as floods linked to human activities), soil dynamics and its rainfall relationship at millennial to decadal scales. Also, records of the Earth's magnetic field using speleothems with good reproducibility have been used to constrain the evolution and dynamics of the field at timescales from excursions to secular variations. In this talk, we will be exploring the mechanisms of the speleothem formation (karst system), the main minerals that are formed and how these processes can impact the magnetic remanence acquisition."

BiCEP and TROUT: Objective Methods for Reanalysis of MagIC Measurement Data

Brendan Cych - University of Liverpool

Paleomagnetic data can be used to make inferences about the Earth core dynamics and plate tectonics over geological timescales. However, many natural samples contain non-ideal magnetic recorders which do not record a consistent magnetization over these timescales. These rocks may produce data which are difficult to interpret. The paleomagnetic community's understanding of non-ideal recorders has improved over time, potentially changing the interpretation of legacy data. However, these data are not always publicly available, leading researchers to include/exclude data based on qualitative criteria such as the Q criteria (doi:10.1016/0040-1951(90)90116-P) for paleomagnetic poles or the QPI criteria (doi:10.3389/feart.2014.00024) for paleointensities. The MagIC database enables researchers to make their data publicly available for reanalysis. Here we present two statistical methods which can be used to reanalyze hard to interpret legacy paleomagnetic data.

The Thermal Resolution of Unblocking Temperatures method (TROUT, Cych et al. in prep) is an approach for analyzing multi-component demagnetization data where the unblocking temperature or coercivity distributions of the magnetic components overlap. TROUT can automatically determine temperature steps to use to isolate a magnetization acquired in a single field for paleodirection and intensity experiments. Additionally it can be used to automatically find the temperature to which a rock was reheated or rotated, for use in studies of pyroclastic emplacement temperatures and baked contact tests.

Bias Corrected Estimation of Paleointensity (BiCEP, doi:10.1029/2021GC009755) is a new approach for estimating paleointensities from Thellier-type experiments. Rather than excluding specimens based on whether they pass or fail a set of subjectively chosen "Selection Criteria", BiCEP assumes an intrinsic relationship between a the "Arai plot curvature" criterion and bias, and uses this to make an unbiased estimate of the paleointensity. BiCEP produces statistically robust error bars which depend on the number of specimens used for the paleointensity estimate and the quality of the data, allowing for consistent analyses of legacy paleointensities.

A global apparent polar wander path for the last 320 Ma calculated from site-level paleomagnetic data

Bram Vaes, **Douwe J.J. van Hinsbergen**, Suzanna H.A. van de Lagemaat, Erik van der Wiel, Nalan Lom, Eldert L. Advokaat, Lydian M. Boschman, Leandro C. Gallo, Annika Greve, Carl Guilmette, Shihu Lie Peter C. Lippert, Leny Montheil, Abdul Qayyum, Cor G. Langereis

Apparent polar wander paths (APWPs) calculated from paleomagnetic data describe the motion of tectonic plates relative to the Earth's rotation axis through geological time, providing a quantitative paleogeographic framework for studying the evolution of Earth's interior, surface, and atmosphere. Previous APWPs were typically calculated from collections of paleomagnetic poles, with each pole computed from collections of paleomagnetic sites, and each site representing a spot reading of the paleomagnetic field. It was recently shown that the choice of how sites are distributed over poles strongly determines the confidence region around APWPs and possibly the APWP itself, and that the number of paleomagnetic data used to compute a single paleomagnetic pole varies widely and is essentially arbitrary. Here, we use a recently proposed method to overcome this problem and provide a new global APWP for the last 320 million years that is calculated from simulated site-level paleomagnetic data instead of from paleopoles, in which spatial and temporal uncertainties of the original datasets are incorporated. We provide an updated global paleomagnetic database scrutinized against quantitative, stringent quality criteria, and use an updated global plate motion model. The new global APWP follows the same trend as the most recent pole-based APWP but has smaller uncertainties. This demonstrates that the first-order geometry of the global APWP is robust and reproducible, indicating that paleomagnetism provides a reliable reference frame as basis for reconstructing, for instance, paleogeography and paleoclimate. Moreover, we find that previously identified peaks in APW rate disappear when calculating the APWP from site-level data and correcting for a temporal bias in the underlying data. Finally, we show that a higher-resolution global APWP frame may be determined for time intervals with high data density, but that this is not yet feasible for the entire 320-0 Ma time span. Future collection of large and well-dated paleomagnetic datasets from stable plate interiors are needed to improve the quality and resolution of the global APWP, which may contribute to solving detailed Earth scientific problems that rely on a paleomagnetic reference frame.

Going virtual: constructing APWPs from VGPs

Mathew Michael Domeier

"Our understanding of Earth's paleogeography relies heavily on paleomagnetic apparent polar wander paths (APWPs), which represent the time-dependent position of Earth's spin axis relative to a block of lithosphere. However, conventional approaches to APWP construction have some potentially significant limitations. First, the paleomagnetic record features substantial noise that is not fully integrated into APWPs. Second, parametric assumptions are adopted to represent spatial and temporal uncertainties even though the data do not always conform to the assumed distributions. The consequences of these limitations remain largely unknown. Here, we overcome these limitations with a bottom-up Monte Carlo uncertainty propagation scheme that operates on site-level paleomagnetic data. To demonstrate our methodology, we present a compilation of site-level Cenozoic paleomagnetic data from North America, which we use to generate a high-resolution APWP. Our results demonstrate that even in the presence of substantial uncertainty, polar wandering can be assessed with unprecedented temporal and spatial resolution."

An integrated magnetic approach to solving the Greater India problem

Stuart Gilder (LMU-Munich) and Jun Meng (CUG-Beijing)

Greater India is part of the Indian plate that was subducted under Asia. Knowing the original surface area of Greater India is a key parameter to define the kinematics of the India-Asia collision, arguably one of the most important tectonic events to shape our planet in the Cenozoic. However, several decades of research have led to gaping discrepancies concerning both the size of the Indian plate in a Gondwanaland configuration and the tectonic history of India, which includes its collision with Asia and the subsequent creation of the Tibetan Plateau. Paleomagnetism and the underlying origin of the magnetic carriers (rock magnetism) lie at the heart of the controversy. Our presentation will introduce the Greater India problem and highlight approaches to solving this paleomagnetic puzzle.

New perspectives on Laurentia's Grenville Loop: tracking Rodinia across the Mesoproterozoic to neoproterozoic boundary

Yiming Zhang

University of California, Berkeley

The paleogeography of Laurentia throughout the Neoproterozoic is critical for reconstructing global paleogeography due to its central position in the supercontinent Rodinia. We develop a new paleomagnetic pole from red siltstones of the early Neoproterozoic Jacobsville Formation which is now constrained to be ca. 990 Ma in age. High-resolution thermal demagnetization experiments resolve detrital remanent magnetization. These remanence directions held by hematite pass an intraclast conglomerate test, giving confidence that the magnetization is detrital and primary. An inclination-corrected mean pole paleomagnetic position for the Jacobsville Formation confirms continued plate motion of Laurentia across the equator in the late Mesoproterozoic to early Neoproterozoic. Laurentia's motion slowed down significantly following the onset of the Grenvillian orogeny. The distinct position of this well-dated pole from those acquired during exhumation and cooling in the Grenville Province that have been assigned a similar age indicates that the ages of the Grenville poles need to be revised to be younger. We use inverted cooling history models based on new apatite U-Pb ID-TIMS thermochronological data to obtain quantitative estimates on the cooling rate and timing of magnetic remanence acquisition for the Adirondack Highlands of the Grenville Province.

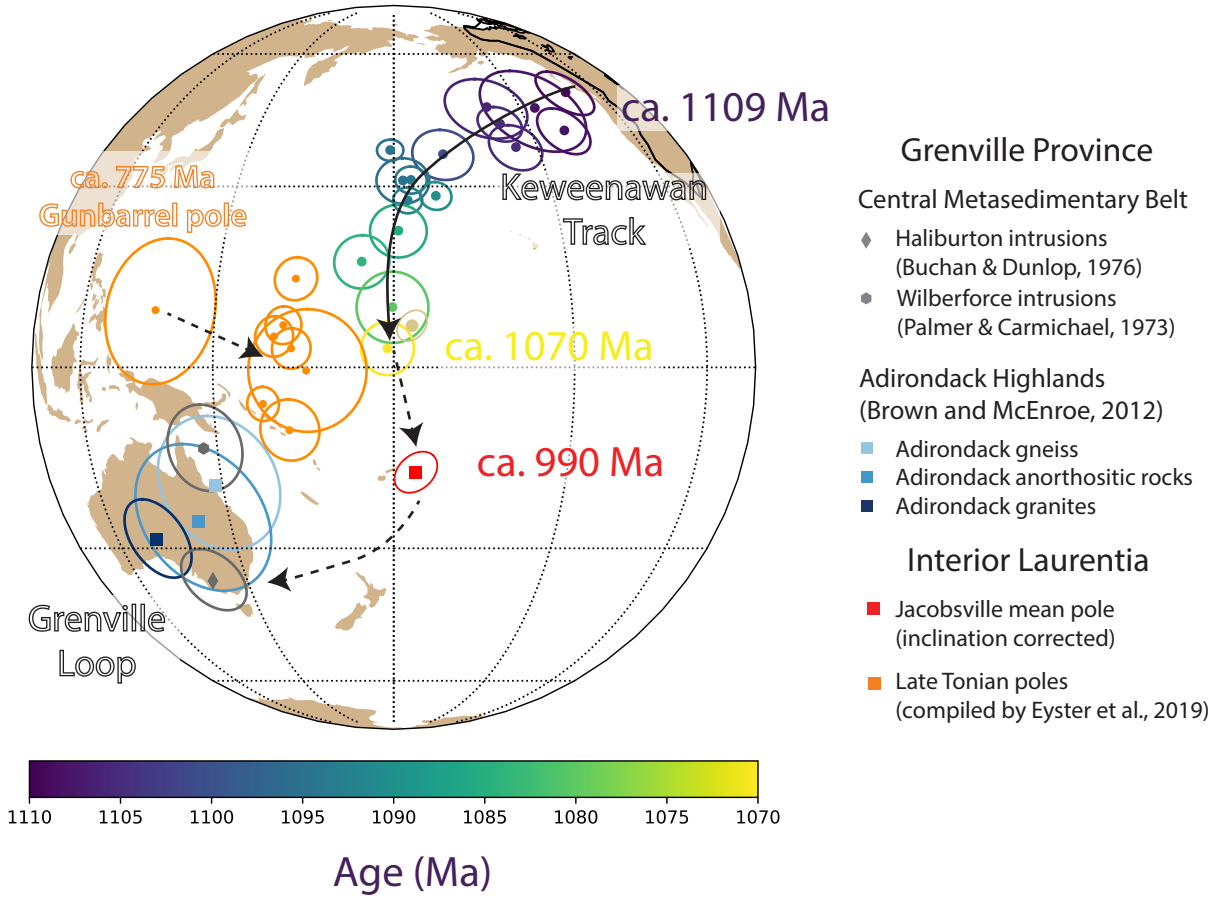
ca. 1109 Ma
ca. 775 Ma
Gunbarrel pole
Keweenawan
Track
ca. 1070 Ma
ca. 990 Ma
Grenville
Loop
1110
1105
1100
1095
1090
1085
1080
1075
1070
Age (Ma)
Grenville Province
Central Metasedimentary Belt
Haliburton intrusions
(Buchan & Dunlop, 1976)
Wilberforce intrusions
(Palmer & Carmichael, 1973)
Adirondack Highlands
(Brown and McEnroe, 2012)
Adirondack gneiss
Adirondack anorthositic rocks
Adirondack granites
Interior Laurentia
Jacobsville mean pole
(inclination corrected)
Late Tonian poles
(compiled by Eyster et al., 2019)

Relationships between lithology and magnetic properties derived from the IODP database

GARY D. ACTON[1] AND LAUREL B. CHILDRESS[2]

Texas A&M University
International Ocean Discovery Program
1000 Discovery Drive
College Station, TX 77845, USA
[1]acton@iodp.tamu.edu
[2]childress@iodp.tamu.edu

We use the **LI**MS With **L**itholog**Y** (**LILY**) database compiled by Childress et al. (in prep.) to examine relationships between magnetic properties and the lithology of marine drill cores collected by the International Ocean Discovery Program (IODP) and its precursor program on Expeditions 318-379. Within LILY, lithologic information such as the principal lithologic name and the major and minor lithologic modifiers, along with other metadata, have been added to each observation in the standard data available in IODP's LIMS Database, which is accessible through the LIMS Online REport (LORE) portal (web.iodp.tamu.edu/LORE/). The ability to compare and combine descriptive lithologic information across expeditions and to integrate these descriptions with multisensor track and discrete sample measurements allows for a wealth of scientific investigation not possible under the original data structure. One of the obvious values of LILY is the ability to characterize the basic physical, chemical, and magnetic properties of different lithologies from a very large number of observations. LILY contains tens of millions of data. For example, there are over 4 million susceptibility measurments made on whole-round core sections with a Bartington MS2C loop and another 3 million susceptibility measurements made on the faces of split-core sections with a Bartington MS2E susceptibility probe. Similarly, remanent magnetization measurements include 6.5 million measurements made on split-core sections with 2G longcore magnetometers and another 65 thousand discrete sample measurements made with spinner magnetometers or longcore magnetometers. As an example of the use of LILY, one might enquire about the mean susceptibility of silt, for which there are over 76,000 whole-round susceptibility measurements. Like the "answer to life, the universe and everything" (Adams, 1979), the susceptibility is 42, at least in raw meter units, which equates to a susceptibility of 2.9×10^{-4} SI Volume.

References:

Childress, L.B., Acton, G.D., Percuoco, V.P., and Hastedt, M., Mining the IODP Database for Relationships Between Lithology and Physical, Chemical, and Magnetic Properties, in preparation.

Adams, D., 1979. The Hitchhiker's Guide to the Galaxy. Pocket Books. ISBN 0-671-46149-4.

Paleomagnetism in the Devils Garden: Mapping basalts on the Modoc Plateau in Northeastern California with directional correlation and anisotropy of magnetic susceptibility

Margaret S. Avery[1*], Anthony F. Pivarunas[1,2], Duane E. Champion[2], Julie Donnelly-Nolan[2]

[1]U.S. Geological Survey, Geology, Minerals, Energy, and Geophysics Science Center

[2]U.S. Geological Survey, Volcano Science Center, California Volcano Observatory

---

The Devils Garden is a large tholeiitic basalt field in northeastern California of Pliocene to Pleistocene age (Luedke and Lanphere, 1980; Hart et al., 1984; Donnelly-Nolan and Lanphere, 2005; Carmichael et al., 2006), located directly east of the Medicine Lake volcano and east of the Cascade volcanic arc in the westernmost Basin and Range extensional province. Its geochemistry indicates a primitive mantle source with little crustal contamination, specifically originating near the crust-mantle boundary from dry decompression melting of shallow mantle (Elkins Tanton et al., 2001). The field comprises isolated older volcanic edifices subsequently engulfed by the voluminous basalts constructing the remarkably flat plateau-top upland topography characteristic of the Modoc Plateau. The highest points on the flat Modoc Plateau topography are old volcanic edifices, the flat plateau topography is disrupted by numerous low-offset Quaternary normal faults.

The size and type of vent sources for the Devils Garden Basalt—shields or fissures—have little topographic expression, suggesting low lava viscosity and rheology that remained essentially uniform over the period of its accumulation. Geochemically they display little variation and all plot in the tholeiitic field. Probing the evolution of this large-volume and spatially distributed volcanic system requires a combination of geological and geophysical techniques. Here we continue the work of Donnelly-Nolan and others (1996) who characterized the "Hackamore basalts" in the western part of the region, adding new sites further east on the Modoc Plateau as well as measuring magnetic anisotropy on archival specimens. Our paleomagnetic directional studies provided precise correlations of lava flows and estimates of eruption duration. We measured anisotropy of magnetic susceptibility to determine lava flow directions (Cañón-Tapia et al. 1996), in cases where a significant anisotropy signal was found, to help trace flows to source vents.

Our paleomagnetic results from the Modoc Plateau region provide detailed information about the evolution of this back-arc basaltic system. We find both normal and reversed characteristic remanent magnetization directions, each of which can be further delineated into flow and unit boundaries. At a broader-scale, we describe three spatially correlated polarity groups, from the normal polarity basalts (dated at 0.629± 0.176 Ma, Donnelly-Nolan and Lanphere, 2005) near the "basalt of Damons Butte" on the western side of the plateau eastward to reversed polarity basalts near the "basalt of Badger Wells" (dated at 1.086 ± 0.026 Ma, Donnelly-Nolan and Lanphere, 2005), and then to the southeastern-most mapped Devils Garden Basalts which are normal polarity (dated between 2.78 and 4.61 Ma, Carmichael et al., 2006). We conclude that the Modoc Plateau lava flows generally young progressively westward and record the Brunhes (normal, 0 – 0.773 Ma), Matuyama (reverse, 0.773 – 2.58 Ma), and Gauss (normal, 2.58 – 3.60 Ma) polarity chrons. Isotopic ages for a targeted selection of several flows will provide a test of this hypothesis.

References

Cañón-Tapia, E., Walker, G. P., & Herrero-Bervera, E. (1996). The internal structure of lava flows—insights from AMS measurements I: near-vent a'a. Journal of Volcanology and Geothermal Research, 70(1-2), 21-36.

Carmichael, I. S., Lange, R. A., Hall, C. M., & Renne, P. R. (2006). Faulted and tilted Pliocene olivine-tholeiite lavas near Alturas, NE California, and their bearing on the uplift of the Warner Range. Geological Society of America Bulletin, 118(9-10), 1196-1211.

Donnelly-Nolan, J.M., Smith, J.G., Champion, D.E., and Lanphere, M.A. (1996). A Pleistocene back-arc basalt center, northeastern CA [abs.]: Geological Society of America Abstracts with Programs, 28(5), 62.

Donnelly-Nolan, J.M., and Lanphere, M.A. (2005). Argon dating at and near Medicine Lake volcano, California—Results and data: U.S. Geological Survey Open-File Report 2005–1416, p.37.

Elkins Tanton, L. T., Grove, T. L., & Donnelly-Nolan, J. (2001). Hot, shallow mantle melting under the Cascades volcanic arc. Geology, 29(7), 631-634.

Hart, W. K., Aronson, J. L., & Mertzman, S. A. (1984). Areal distribution and age of low-K, high-alumina olivine tholeiite magmatism in the northwestern Great Basin. Geological Society of America Bulletin, 95(2), 186-195.

Luedke, R. G., & Lanphere, M. A. (1980). K–Ar ages of Upper Cenozoic volcanic rocks, northern California. Isochron/West, 28, 7-8.

An assessment of zonal drift in the paleomagnetic field for the past 100 kyr

Nicole Clizzie & Cathy Constable
University of California San Diego, Scripps Institution of Oceanography
Institute of Geophysics & Planetary Physics

February 6, 2023

The Earth's magnetic field changes spatially and across time scales; these changes are called geomagnetic and paleomagnetic secular variations. A well-known secular variation feature is westward drift, while a less prominent feature is eastward drift. Previous studies used time-varying paleo(geo)magnetic field models gufm1 (1590-1990), CALS7k.2 (0-7 ka), and pfm9k.1a (0-9 ka) to track zonal (azimuthal) motion of the radial magnetic field by performing Radon drift determination and frequency-wavenumber analyses on time-longitude plots. In this study, we extended such analyses by using global geomagnetic field models covering the past 100 ka. The models are GGF100k (0-100 ka), GGFSS70 (15-70 ka), LSMOD.2 (30-50 ka), and all of them include the Laschamp excursion (40-42 ka) with varying degrees of resolutions. GGFSS70 and LSMOD.2 both have higher temporal resolution than GGF100k. We found recurrent episodes of both eastward and westward drift ranging from $\pm 0.05 \frac{^0}{year}$ to $\pm 0.18 \frac{^o}{year}$ in both the northern (Figure 1 middle and right panels) and southern hemispheres. We also found 10-20 kyr intervals of high-latitude reverse flux patches, which correlate with high-frequency drift signals.

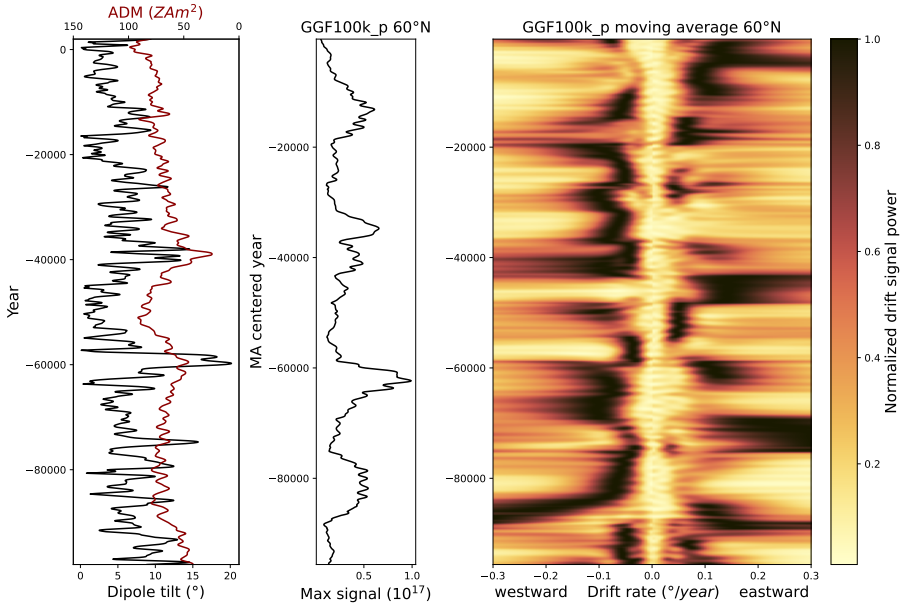

Figure 1: Paleomagnetic model: GGF100k. left panel: the black line is the dipole tilt, and the brown line is the axial dipole moment (ADM). The ADM axis is reversed. Right panel: Radon drift moving average from a time-longitude plot with a 4000-year time-drift window and with 100-year increments. The time-longitude plot (60°N) was calculated using a high pass Butterworth ($f_c = \frac{1}{4000yrs}$) filter on the Gauss coefficients with the time-averaged axisymmetric parts of the field removed. Middle panel: The maximum signal power is the normalizing signal power in each time window for the Radon drift moving average (right panel).

The EPOS Multi-scale laboratories – MagIC connection: lessons learned from connecting repositories to portals

Kirsten Elger[1*], Otto Lange[2], Geertje ter Maat[2], Laurens Samshuijzen[2]

1. *GFZ German Research Centre for Geosciences, Potsdam, Germany*
2. *Utrecht University, Utrecht, The Netherlands*

The EPOS Multi-scale Laboratories (MSL) are a network of European laboratories bringing together the scientific fields of analogue modeling, paleomagnetism, experimental rock and melt physics, geochemistry and microscopy (Figure 1, Elger et al., 2022). MSL is one of nine Thematic Core Services (TCS) of the European Plate Observing System (EPOS). The overarching goal of EPOS is to establish a comprehensive multidisciplinary research platform for the Earth sciences in Europe. It aims at facilitating the integrated use of data, models, and facilities, from both existing and new distributed pan European Research Infrastructures, allowing open access and transparent use of data.

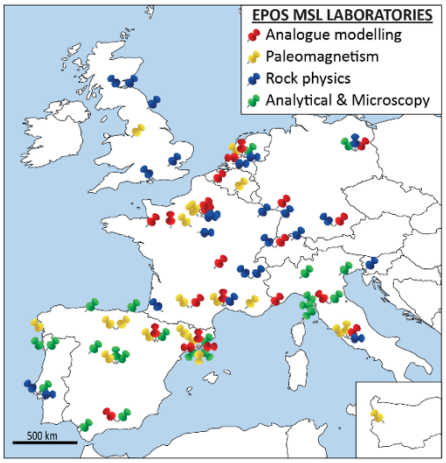

Figure 1: Map of European solid Earth laboratories in Europe and their domains. (Figure from Elger et al., 2022)

Data from Multi-scale Laboratories can be described as "long-tail" of research data. These data are small in terms of memory size but highly variable, hence difficult to standardize and curate. But they represent a large portion of the total quantity of research data. To include these data from European laboratories in the EPOS infrastructure, we have developed the following strategy: DOI-referenced data publications via domain repositories have been identified as best practice for "FAIR" sharing data, especially in long-tail communities with highly variable data types: researchers are describing their data via metadata editors that convert the information to standardized and machine-readable metadata formats (XML, JSON). These are made available via standard application programming interfaces and/ or embedded in the web-sites (Schema.org) by the repository. Data curation by domain scientists, a rich metadata schema that includes several controlled linked-data vocabularies, and additional technical description via data description templates further improve the quality of the published data and their documentation.

The EPOS Multi-scale laboratories have explicitly decided to not develop any new data repository for data from European laboratories data, but, instead, partner with existing domain-repositories that publish curated data with DOI and that are successively connected to the newly developed MSL Portal (LINK). Together with the partner repositories, MSL offers researchers a fully operational data publication chain tailored to the specific needs of laboratory research, from a bespoke metadata editor, through dedicated, FAIR-aligned (domain-specific) data repositories, to the MSL Portal showcasing these data publications (Figure 2). During this process the data publications are assigned with DOI and published with open licenses (e.g. CC BY 4.0). This makes research data Findable, Accessible, Interoperable, Reusable (FAIR, Wilkinson et a., 2016) and citable for other scientists.

The main partner repository is GFZ Data Services, the domain repository for Geosciences data, hosted at the GFZ German Research Centre for Geosciences. GFZ Data Services is open for all MSL

Figure 2: Illustration of the MSL data publication chain for collecting rich metadata used for DOI-referenced data publications that are harvested to the MSL Portal which itself is connected to the central EPOS portal (Figure from Elger et al., 2022).

data, implemented the dedicated metadata schema and developed the MSL-specific metadata editor. GFZ Data Services has a focus on the curation of long-tail data. The repository implements the FAIR principles (Wilkinson et al., 2016) by

1) the provision of comprehensive domain-specific metadata that integrate controlled "linked-data" domain vocabularies as well as MSL community-derived controlled vocabularies in international metadata standards for data discovery (DataCite, ISO19115);
2) complementing the metadata with detailed data descriptions or reports; and
3) embedding the research data in wider context by providing cross-references through persistent identifiers to related research products and people or institutions involved (DOI, IGSN, ORCID, Fundref, ROR).

To facilitate discovery through internet search engines like Google, all DOI landing pages of GFZ Data Services embed machine-readable metadata following Schema.org and present xml versions of the metadata in DataCite and ISO 19115 standards. The OAI-PMH interface can be queried with search parameters which allows the harvesting of a specific subset. In addition, GFZ Data Services feed links of data and related research products into Scholix, which allows direct linking of data publications and scholarly literature, even when the data are published years after the article.

For paleomagnetic data, the MSL community actively sought to establish an international collaboration with the Magnetics Information Consortium (MagIC), the US-based global paleomagnetic database. This included, on one hand, the general agreement of MagIC to be open for data from European laboratories and joint workshops and tutorials encouraging researchers from European laboratories to publish their data via MagIC. On the other hand, it included the identification of metadata elements from MagIC and their harmonization with the MSL metadata schema as well as agreements on the metadata exchange format. The poster will introduce to the MSL network of European laboratories, GFZ Data Services and describe the challenges and solutions enabling the "MagiC – MSL connection".

References:

Elger, K., ter Maat, G., Caldeira, R., et al. (2022): The EPOS Multi-Scale Laboratories: A FAIR Framework for stimulating Open Science practice across European Earth Sciences Laboratories. - Annals of Geophysics, 65, 3, DM318. https://doi.org/10.4401/ag-8790

Wilkinson, M., M. Dumontier, I. Aalbersberg, I. et al. (2016) The FAIR Guiding Principles for scientific data management and stewardship. Sci Data 3, 160018, https://doi.org/10.1038/sdata.2016.18

Relative Paleointensity in the Pliocene: New perspectives on old questions.

Robert G. Hatfield, Joseph S. Stoner, and Andrew J. Fraass.

Department of Geological Sciences, University of Florida, Gainesville, Florida 32611, USA
College of Earth, Ocean, & Atmospheric Sciences, Oregon State University, Corvallis, Oregon 97331, USA
Earth & Ocean Sciences, University of Victoria, Victoria, British Columbia, Canada.

Long sedimentary records of relative geomagnetic paleointensity (RPI) offer unique insights into geodynamo behavior and can be developed into chronostratigraphic templates capable of (sub-)orbital scale age control. The Quaternary record of RPI has received much attention, but records extending back into the Pliocene are relatively rare. Here we show two new Pliocene-age RPI records from IODP Site U1396 in the Caribbean Sea and from IODP Site U1489 in the western equatorial Pacific Ocean. Paleomagnetic data quality at IODP Site U1396 is closely linked to paleoceanographic changes and the evolution of the Lesser Antilles Volcanic Arc and is best preserved between 2.1 – 4.5 Ma. All 11 polarity reversals are preserved between the top of the Nunivak and the top of the Feni and augmented by a benthic oxygen isotope stratigraphy, sedimentation rates are estimated to average between 4-5 cm/kyr during the Plio-Pleistocene. Discrete intervals of volcanogenic origin punctuate the record, so the normalized intensity record is refined using a multi-step sedimentological, rock magnetic, and paleomagnetic screening process that improves MAD values and tightens the scatter in the directional record. Shallower than GAD inclination observed during reversed polarities cannot easily be explained by rock magnetic variability or a pervasive overprint and may be a characteristic feature of the field during this period (Schneider and Kent, 1990, 1988). At IODP Site U1489 sedimentation rates are lower, averaging ~2 cm/kyr, but all 16 polarity reversals back to the top of the Nunivak are clearly identified. MAD values average ~2°, NRM intensity normalized by magnetic susceptibility and ARM give similar answers, and a continuous RPI-proxy is generated for the past 4.5 Myrs. Despite the differing depositional environments, the RPI records from IODP Sites U1396 and U1489 show coherence to each other, to the EPAPIS and NARPI-2200 RPI stacks, and to RPI records from IODP Sites U1314 and U1308 that span the oldest-Pliocene and Pleistocene (Channell et al., 2016; Hatfield et al., 2021; Ohno et al., 2012; Yamazaki and Oda, 2005). Before ~3 Ma very few records exist for comparison. Of those that do, the composite record from ODP Sites 848/851 exhibits a controversial saw-tooth pattern in RPI while the long 8 Myr record from IODP Site U1335 suggested a baseline increase in paleointensity occurred around 4 Ma (Valet and Meynadier, 1993; Yamazaki and Yamamoto, 2018). Neither of our new records contain evidence to support these previous findings. They do however begin to establish characteristic variability in RPI during periods of stable polarity. For example, in all available records, the interval between the Gilbert-Gauss boundary and the base of the Mammoth, is characterized by a sequence of four RPI-highs and three RPI-lows. This characteristic pattern, if shown to be robust, could provide useful chronological constraints during a middle Pliocene period of increasing interest as global temperature may have been similar to that projected in our near future. The development of these long Pliocene-age records opens the door to extending the success stories of Pleistocene RPI deeper into pre-Quaternary times.

References:
Channell, J.E.T., Hodell, D.A., Curtis, J.H., 2016. Relative paleointensity (RPI) and oxygen isotope

stratigraphy at IODP Site U1308: North Atlantic RPI stack for 1.2-2.2 Ma (NARPI-2200) and age of the Olduvai Subchron. Quat. Sci. Rev. https://doi.org/10.1016/j.quascirev.2015.10.011

Hatfield, R.G., Stoner, J.S., Fraass, A.J., 2021. Relative Paleointensity Record of Integrated Ocean Drilling Program Site U1396 in the Caribbean Sea: Geomagnetic and Chronostratigraphic Observations in the Pliocene. Geochemistry, Geophys. Geosystems 22, e2021GC009677. https://doi.org/10.1029/2021GC009677

Ohno, M., Hayashi, T., Komatsu, F., Murakami, F., Zhao, M., Guyodo, Y., Acton, G., Evans, H.F., Kanamatsu, T., 2012. A detailed paleomagnetic record between 2.1 and 2.75 Ma at IODP Site U1314 in the North Atlantic: Geomagnetic excursions and the Gauss-Matuyama transition. Geochemistry, Geophys. Geosystems. https://doi.org/10.1029/2012GC004080

Schneider, D.A., Kent, D. V., 1990. The time-averaged paleomagnetic field. Rev. Geophys. 28, 71–96. https://doi.org/10.1029/RG028i001p00071

Schneider, D.A., Kent, D. V., 1988. Inclination anomalies from Indian Ocean sediments and the possibility of a standing nondipole field. J. Geophys. Res. 93. https://doi.org/10.1029/jb093ib10p11621

Valet, J.P., Meynadier, L., 1993. Geomagnetic field intensity and reversals during the past four million years. Nature 366, 234–238. https://doi.org/10.1038/366234a0

Yamazaki, T., Oda, H., 2005. A geomagnetic paleointensity stack between 0.8 and 3.0 Ma from equatorial Pacific sediment cores. Geochemistry, Geophys. Geosystems. https://doi.org/10.1029/2005GC001001

Yamazaki, T., Yamamoto, Y., 2018. Relative Paleointensity and Inclination Anomaly Over the Last 8 Myr Obtained From the Integrated Ocean Drilling Program Site U1335 Sediments in the Eastern Equatorial Pacific. J. Geophys. Res. Solid Earth 123, 7305–7320. https://doi.org/10.1029/2018JB016209

Novel Insights into the Palaeomagnetism of Serpentinized Peridotites from the Oman and Troodos Ophiolites.

James Hepworth[1], Antony Morris[1], Michelle Harris[1], Richard Harrison[2], Esther Schwarzenbach[3]

1. School of Geography, Earth and Environmental Sciences, University of Plymouth, UK.
2. Department of Earth Sciences, University of Cambridge, UK.
3. Department of Geosciences, Université de Fribourg, Switzerland

Large volumes of mantle peridotite rocks are exposed at the Earth's surface in ophiolites, becoming vulnerable to the concurrent chemical alteration processes of serpentinization and carbonation. Serpentinization frequently results in the production of secondary magnetite that records the direction of the Earth's magnetic field at the time of its formation, allowing palaeomagnetism to be used as a tool to investigate this process.

Various Late Cretaceous supra-subduction zone Tethyan ophiolites, such as the Samail ophiolite in Oman and the UAE (hereafter referred to as the Oman ophiolite) and the Troodos ophiolite in Cyprus, also show evidence for large-scale tectonic rotation during their evolution. The timing of these rotations is well-documented palaeomagnetically and can be used as a temporal reference framework to date phases of serpentinization occurring at different times if the directions of magnetization of different assemblages of secondary magnetite grains may be determined. This project will therefore take advantage of the recent development of high-resolution magnetic microscopes to analyse individual grain assemblages in serpentinized peridotites for the first time, and to test whether this and other paleomagnetic techniques can successfully resolve the timing of sequential phases of alteration. Both the Oman and Troodos ophiolites underwent very large tectonic rotations after they formed by seafloor spreading (Oman by ~120 CW, Troodos by ~90 CCW). Serpentinization of the mantle peridotites of these ophiolites could potentially have happened during any or all of the following stages in their evolution:

- By exposure on the seafloor or via deep fluid circulation during Late Cretaceous seafloor spreading.
- During tectonic rotation after cessation of seafloor spreading.
- For Oman, during Late Cretaceous emplacement onto the Arabian continental margin.
- For Troodos, during Late Cretaceous to Recent tectonic uplift.
- Via reactions with modern meteoric water (both have alkaline springs that demonstrably relate to ongoing serpentinization).

Because of the very large tectonic rotations of these ophiolites, magnetite assemblages formed by serpentinization at different stages in their evolution should carry different directions of magnetization. Here we present bulk sample palaeomagnetic data from serpentinites from both ophiolites which demonstrate varying palaeomagnetic directions related to rotation of the ophiolites. For Troodos, samples from site 12 display ChRM directions which record the large CCW rotation of the Troodos ophiolite probably acquired during/soon after Late Cretaceous seafloor spreading. For Oman, some samples from site 14 display ChRM directions which record the large CW rotation of the Oman ophiolite, and some samples appear to display partially rotated directions. Future work includes taking advantage of recent advances in Quantum Diamond Microscopy (QDM) to test whether: (1) it can distinguish different generations of secondary magnetite with different palaeomagnetic directions in the same sample and (2) are the low stability, present day field directions (in samples with rotated ChRM directions), a result of viscous overprints in the same grain assemblage or a separate serpentinization event?

Low-temperature magnetic behavior of Apollo mare basalts.

J. Jung[1] (jiinjung@stanford.edu), S. M. Tikoo[1,2], D. Burns[2], S. Channa[3], H. Yang[1,2], [1]Dept. of Geophysics, Stanford University, Stanford, CA 94305; [2]Dept. of Earth and Planetary Sciences, Stanford University, Stanford, CA 94305; [3]Dept. of Physics, Stanford University, Stanford, CA 94305.

The Moon's reducing environment promotes the presence of metallic iron phases within igneous rocks, rather than iron oxides (e.g., magnetite and hematite) commonly observed on Earth [1-4]. During the initial cooling process, the body-centered cubic FeNi alloys kamacite (α-$Fe_{1-x}Ni_x$ for $x < \sim 0.05$) and martensite (α_2-$Fe_{1-x}Ni_x$ for $\sim 0.05 < x < \sim 0.25$) formed in lunar mare basalts. These FeNi grains are typically either embedded within the troilite phase (FeS) in a eutectic assemblage or associated with chromium-ulvospinel (Cr-rich spinel) or titanian-chromite (Ti-rich chromite) [5, 6].

In this study, we investigated the low-temperature magnetic properties of various types of lunar mare basalts (e.g., 10003, 10020, 10044, 10069, 10071, 12022, 15597) as well as Fe alloys and ilmenite ($FeTiO_3$) through Magnetic Property Measurement System (MPMS) experiments. The samples were also subjected to scanning electron microscopy with energy dispersive x-ray spectroscopy (SEM/EDS) and electron probe microanalysis (EPMA) on thin sections. Based on the results of petrographic analysis, samples are classified into three different groups based on the the opaque minerals present: Type 1: FeNi alloys associated with Troilite + Ilmenite (e.g., 10003, 10044, 10069, 10071), Type 2: FeNi alloys associated with Troilite + Ilmenite + Chromium-Ulvospinel (e.g., 10020, 12022), Type 3: FeNi alloys associated with Titanian-Chromite or Silicates (e.g., 15597).

The low-temperature magnetic behavior for all lunar basalts seems to resemble those of Fe alloys showing an increase in a magnetic moment as the temperature decreases. Type 1 and Type 2 samples showed clear phase transitions at ~50 - 60K in field-cooled (FC), and room temperature saturated magnetization (RTsIRM) curves, which is consistent with the Néel transition of troilite at ~ 60 K [7]. Our standard ilmenite sample does not show any signature in low-temperature magnetic remanence, although ilmenite has a Néel transition at ~ 65 K [8]. Interestingly, all samples showed a phase transition at ~120K in FC, zero-field cooled (ZFC), and RTsIRM curves. This phase transition could possibly be chromium-ulvospinel (which has Curie temperature at ~115K) for Type 2 samples and titanian-chromite (which has three possible transitions at 37K, 69K, and 124K [9-10]) for one Type 3 sample.

However, the origin of this transition for Type 1 basalts is unclear. An increase in magnetization at approximately 120 K appears similar to the magnetite Verwey transition [10]. If this is the case, $\delta_{FC}/\delta_{ZFC} > 1$ below the transition suggests that the magnetite grains would likely be the single domain (SD) [11]. Our electron microscopy results revealed trace amounts of oxygen in Fe grains that were associated with troilite. WDS scans of the metallic phase in sample 10071 show distinct peaks for Fe (Lα and Lβ) and oxygen (Kα), indicating between 3 and 4 wt. % oxygen. Identifying this magnetic mineral and its origin will help to understand past lunar environments and/or magnetic carriers in lunar paleomagnetism. Future work will include investigating any possible oxidation processes associated with sample preparation (e.g., dry band saw cutting used to prepare thin sections) and further mineral characterization with various electron microscopy techniques.

References:

[1] Sato M. et al., (1973), *Proc. Lunar Sci. Conf. 4th,* 1061-1079. [2] Sato M. (1976) *Proc. Lunar Sci. Conf. 7th,* 1323-1344. [3] *Haggerty S. E. (1978) GRL*, 5, 443-446. [4] Tikoo S. M, and A. J. Evans., (2021) *Annu. Rev. Earth. Planet. Sci., 50:1*, 99-122. [5] Skinner B., (1970) *Sci., 167*, 3918. [6] Cameron E. (1970), *Proc. Lunar Sci. Conf. 4th,* 221-245. [7] Kohout T. A. et al., (2007) *EPSL, 261*, 131-151. [8] Senftle P. A. et al., (1975) *EPSL, 26,* 377-386.[9] Klemme S. et al., (2000) *Ame Min*, *85*, 1686-1693. [10] Gattacceca J. et al., (2011) *GRL, 38*, L10203. [11] Moskowitz B. M. et al., (1993) *LPSC, 120,* 283-300.

On the possibility of a complete Ediacaran field collapse

Kenneth P. Kodama[1], Tinghong Zhou[2], Richard K. Bono[3], Rory D. Cottrell[2], John A. Tarduno[2,4,5]

[1] Department of Earth and Environmental Sciences, Lehigh University, Bethlehem, PA 18015, USA
[2] Department of Earth & Environmental Sciences, University of Rochester, Rochester, NY, 14627 USA
[3] Department Earth, Ocean and Atmospheric Science, Florida State University, Tallahassee, FL 32306, USA
[4] Department of Physics & Astronomy, University of Rochester, Rochester, NY, 14627 USA
[5] Laboratory for Laser Energetics, University of Rochester, Rochester, NY, 14623, USA

In the past decade there has been increased multidisciplinary interest in the onset time of inner core nucleation (ICN). Biggin et al. (2015) suggested a Mesoproterozoic age based on apparent high field values in the paleointensity database. Smirnov et al. (2016) subsequently pointed out that some of these high values were derived from studies where viscous remanent magnetization likely contaminate any primary remanence, leading to paleointensity overestimates. Arguably, the most obvious example of this is the appearance of single slope Arai plots, starting at very low unblocking temperatures (less than 100 ^{o}C). Given that nearly all the rocks defining the Mesoproterozoic high fields in the database contain multidomain grains, it is impossible for low unblocking temperatures to be free of overprints acquired in the present-day field, or over the more than 1 billion years of history since their formation. This was emphasized in the restudy of the Gardar basalts by Kodama et al. (2019), who were unable to duplicate the high field values and concluded there was no evidence for a Mesoproterozoic ICN age.

Another major step forward toward understanding ICN from paleomagnetism was the discovery by Bono et al. (2019) of ultralow fields in Ediacaran-age (565 Ma) anorthosites of the Sept Îles layered mafic sequence of northern Quebec, Canada. These results were based on single crystal paleointensity data (feldspars and pyroxene) with ideal single domain magnetic carriers documented by magnetic hysteresis, first order reversal curve data, and scanning electron microscopy. By virtue of the relatively slow cooling of the anorthosite sampled the ultralow value- some ten times less than the present-day field - was time averaged. Independent thermal and numerical dynamo modeling by Driscoll (2016) predicted the weak-field state prior to ICN. Bono et al. (2019) combined the unusual magnetic behavior (e.g., a hyper-reversal state) from global studies together with the Sept Îles ultra-low field value to suggest ICN near 565 Ma. Another observation made by Bono et al. (2019) was a possible trend - with superimposed variations - from Archean high intensities to the Ediacaran ultralow value. Variations are expected, representing changes in core-mantle boundary boundaries, as invoked for the Mesozoic (Glatzmaier et al., 1999; Tarduno et al., 2002). But nevertheless, a long-term signal matching model predictions leading to ICN was present in select (Thellier) time-averaged values. Another salient suggestion made by Bono et al. (2019) was that the Ediacaran Period might mark the start of quasi-200 million-year long cycles in paleointensity. Subsequently, Ediacaran ultralow fields have been reported from several paleointensity studies of dikes (Shcherbakova et al., 2020; Thallner et al., 2021). Although relatively few Thellier results are available, these nevertheless indicate the presence of ultralow fields from multiple cratons, providing an important global consistency test.

Zhou et al. (2022) have recently reported a field strength 5 times higher than the Ediacaran ultralow field value in a single crystal paleointensity (feldspar) study of 532 Ma anorthosite of Oklahoma. A preliminary study of whole rock paleointensity at Lehigh University yields

similar values. We interpret this early Cambrian gain in field strength to be a signature of new energy sources to power the dynamo accompanying inner core growth. Other times continue to be proposed for the time of ICN, but the Ediacaran Period stands apart in its evidence for time-averaged ultralow fields consistent with independent predictions from thermal and numerical dynamo models (Davies et al., 2022).

With this background, we consider whether the internally generated field did not just decline to ultra-low values but might have effectively disappeared for some time interval of the Ediacaran Period. We study whole rock paleointensity values from Ediacaran-age dikes originally samples by R.K.B. and J.A.T. in November of 2014 as part of their field studies in Canada (e.g., Bono and Tarduno, 2015). We find Arai plots with extreme two-slope behavior. The low temperature slope appears to be a thermo-viscous overprint, whereas the high temperature slope, if interpreted as a viable paleointensity measure, records ultra-low fields. The whole rocks almost certainly contain some large multidomain grains. Here we investigate the possibility that the high temperature slope is a field overestimate, reflecting not the true ambient field but rather the dominant viscous overprint that has contaminated higher unblocking temperatures. If correct, it is further possible that this overprint might be concealing even lower ambient fields, or a complete collapse of the dynamo. We will discuss our plans to experimentally assess this hypothesis.

This work was supported by NSF grants 1828825 (K.P.K.) and 1828817 (J.A.T.).

References

Biggin, A. J., et al. Palaeomagnetic field intensity variations suggest Mesoproterozoic inner-core nucleation. *Nature* **526**, 245-248 (2015).

Bono, R.K. & Tarduno, J.A. Stable Earth, reversing field in the Ediacaran: A single silicate crystal study of the ca. 565 Ma Sept-Îles Intrusive Suite in Laurentia, *Geology*, **43**, 131-134 (2015).

Bono, R. K., Tarduno, J. A., Nimmo, F. & Cottrell, R. D. Young inner core inferred from Ediacaran ultra-low geomagnetic field intensity. *Nat. Geosci*. **12**, 143-147 (2019).

Davies, C. J., et al., Dynamo constraints on the long-term evolution of Earth's magnetic field strength, *Geophys. J. Inter*. **228**, 316-336 (2022).

Driscoll, P. Simulating 2 Ga of geodynamo history. *Geophys. Res. Lett.* 43, 5680-5687 (2016).

Glatzmaier, G. A., Coe, R. S., Hongre, L. & Roberts, P. H. The role of the Earth's mantle in controlling the frequency of geomagnetic reversals. *Nature* **401**, 885-890 (1999).

Kodama, K.P., Carnes, L.K., Tarduno, J.A. & Berti, C., Paleointensity of the 1.3 billion-yr-old Gardar basalts, southern Greenland revisited: no evidence for onset of inner core growth, *Geophys. J. Inter.*, **217**, 1974-1987 (2019).

Shcherbakova, V.V., et al. Ultra-low palaeointensities from East European Craton, Ukraine support a globally anomalous palaeomagnetic field in the Ediacaran. *Geophys. J. Int*. **220**, 1920–1946 (2020).

Smirnov, A. V., Tarduno, J. A., Kulakov, E. V., McEnroe, S. A. & Bono, R. K. Palaeointensity, core thermal conductivity and the unknown age of the inner core. *Geophys. J. Inter*. **205**, 1190-1195 (2016).

Tarduno, J. A., Cottrell, R. D. & Smirnov, A. V. The Cretaceous Superchron geodynamo: Observations near the tangent cylinder. *Proc. Nat. Acad. Sci. USA* **99**, 14020-14025 (2002).

Thallner, D., Biggin, A. J. & Halls, H. C. An extended period of extremely weak geomagnetic field suggested by palaeointensities from the Ediacaran Grenville Dykes (SE Canada). *Earth Planet. Sci. Lett.* **568**, 117025 (2021).

Zhou, T., et al. Early Cambrian renewal of the geodynamo and the origin of inner core structure. *Nat. Commun*. **13**, 4161 (2022).

Identification of Ferromagnetic Phases in Perseverance Rover Samples and Implications for Paleomagnetic Analysis of Returned Samples

E. N. Mansbach[1], T. V. Kizovski[2], L. Mandon[3], E. L. Scheller[1], T. Bosak[1], R.C. Wiens[4], C. D. K. Herd[5], B. P. Weiss[1], [1]Massachusetts Institute of Technology (MIT), Cambridge, MA, USA, [2]Brock University, Toronto, Canada, [3]California Institute of Technology, Pasadena, CA, USA, [4]Purdue University, West Lafayette, IN, USA, [5]University of Alberta, Edmonton, Canada.

Introduction and Methods: While Mars does not have a dynamo today, the identifications of remanent magnetization in Martian meteorites (ALH 84001, ~4 Ga) [1] and in the Martian crust [2] indicate that Mars once possessed an internally generated magnetic field. A key unknown about the ancient dynamo is its lifetime, which analyses of crustal magnetization suggest to be 4.5 – 3.7 billion years (Ga) ago [3]. However, the true lifetime of the dynamo is uncertain as it could have decayed after 3.7 Ga and the ages of the crustal anomalies are often based on poorly constrained crater counting methods. Determining the lifetime of the Martian dynamo is vital to understanding the evolution of the Martian interior (thermochemical history of the core and mantle) and the potential habitability of the planet (role of the dynamo in loss of the early atmosphere and surface water) [4].

The Perseverance rover is currently exploring a delta in the Jezero impact crater at the edge of the Isidis basin [5]. The delta is emplaced on top of the crater floor, which consists of two formations: an olivine cumulate (Séitah) overlain by a basalt (Máaz) [6]. Near the contact with the crater floor, the delta consists of sedimentary units comprising sand-sized and sand-to-silt-sized grains. A primary goal of the Perseverance rover is to collect samples that will be returned to Earth in the early 2030s. Unlike our current inventory of Martian meteorites, these samples will have known geologic contexts, are almost all oriented bedrock samples, and will not have experienced terrestrial weathering or collectors' hand magnets. Given the suggested age of the delta and future exploration outside the crater rim, the samples are expected to range in age from ~2 to >4.1 Ga [5]. Thus, the samples likely record the intensity and direction of the Martian dynamo during its early history and its decline. In order to understand the paleomagnetic record of the returned samples, we will need to determine their ferromagnetic mineralogy, the form of their natural remanent magnetization (NRM), and the grain sizes of the phases. For the crater floor, which is igneous in origin, and the delta, which is sedimentary, possible remanence acquisition methods include: (1) thermoremanent magnetization (TRM) during cooling, (2) chemical remanent magnetization (CRM) during aqueous alteration, and (3) detrital remanent magnetization (DRM) during grain transport and deposition. Determining the form of the samples' NRMs is vital as a TRM would provide an opportunity to measure a reliable paleointensity, while DRMs or CRMs could provide a continuous record of the Martian magnetic field. Quantifying the grain sizes of any ferromagnetic phases will provide an indicator of domain states and determine whether any magnetization could be retained over Ga-scale timeframes.

Here, we provide a first look at what ferromagnetic phases exist in the samples collected thus far, what magnetizations these samples are likely to retain, and implications for future analysis of the returned samples. We synthesize data from the Planetary Instrument for X-Ray Lithology (PIXL) [7] and SuperCam [8] instruments. PIXL uses X-ray fluorescence (XRF) to create high-resolution elemental maps which allows us to identify regions enriched in elements commonly found in magnetic phases (Fe, Ti, Cr). SuperCam measures elemental compositions using laser induced breakdown spectroscopy (LIBS) and can collect visible and near-infrared spectra (VISIR) to identify mineralogy.

Results: In the crater floor, PIXL scans of Séitah abrasion patches (Fig. 1a) show regions enriched in Fe, Ti, and Cr [9]. The Fe- and Cr-enriched regions are located within individual olivine and pyroxene grains, while the Fe- and Ti-enriched regions occur in the surrounding mesostasis. Due to grain signal mixing, we cannot determine the stoichiometry of the iron oxides. However, we propose that the Fe- and Cr-enriched regions are either chromite or a Cr-magnetite, and the Fe- and Ti-enriched regions may be indicative of titanomagnetite or ilmenite. Note that both chromite and ilmenite are not ferromagnetic at room temperature. Collocating the identified iron-oxide regions in color images of the scan areas, we see that the identified iron oxides align with dark-colored grains that are ~350 μm in size (Fig. 1b). These

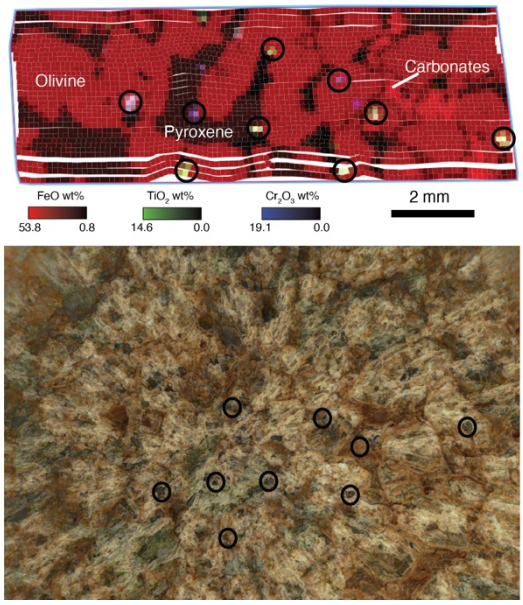

Figure 1: *Top*: PIXL map of the Dourbes (Seitah) abrasion patch. Yellow/green spots are Fe-Ti oxides, white spots are Fe-Ti-Cr oxides, and blue/purple spots are Cr-rich oxides. Potential iron oxides are circled in black. *Bottom*: Colorized ACI image of the abrasion patch. The circles show the locations of the potential iron oxides in the PIXL scan.

grains, if they are magnetite, are likely multidomain on account of their size [10]. VISIR spectra indicate the presence of nonferromagnetic ferrihydrite [11], while normative mineral compositions from LIBS imply 1.6 wt% magnetite and 1.1 wt% ilmenite in the formation [12].

PIXL scans of the Máaz formation show no Cr-enriched oxides. However, there are twice the number of locations enriched in Ti and Fe compared to Séitah. These regions may be titanomagnetite or ilmenite. VISIR spectra indicate the presence of iron oxyhydroxides while normative mineral compositions from LIBS imply 1.8 wt% magnetite and 0.4 wt% ilmenite in the formation [12, 13].

In the delta front, only one spot in the Thorton Gap abrasion patch (Skinner Ridge Sandstone) PIXL scan exhibits enrichment in Fe, Ti and Cr and may be a Cr-rich titanomagnetite. VISIR spectra in the Amalik and Devils Tanyard members possibly detect magnetite [13].

Discussion: The igneous texture of the crater floor formations and the primary nature of the mafic silicates indicate that if titanomagnetite is present, it would have acquired a TRM during primary cooling. However, there is evidence that the rocks have been altered by a fluid [14], and therefore additional analysis on Earth will be needed to determine if the rocks acquired a secondary CRM. These formations are the oldest that the rover has currently sampled, but their potential ~3.8 Ga age [15] is still older than the youngest putative evidence for a dynamo. Therefore, these samples may not constrain the timing of dynamo cessation but would constrain the paleofield intensity and direction.

Additional analyses on rover data are required to determine the presence of iron oxides in the delta samples. The only unambiguous detection of an iron oxide in the Thorton Gap abrasion patch has an uncertain remanence acquisition method. If the grain is detrital in origin, it may carry a TRM acquired during initial cooling in the Jezero watershed >4 Ga. However, the average size of the grains in the abrasion patch (~250 μm) suggests that if a field was present, the grain could have acquired a DRM during deposition (3.6-3.8 Ga) [16, 17]. Since this timeframe spans the youngest evidence for a dynamo, these delta samples and future, younger samples, could aid in constraining the time of dynamo cessation. Alternatively, the grain could have formed during aqueous alteration, acquiring a grain-growth CRM.

Conclusion: The identification of iron oxides in multiple formations studied by Perseverance suggests that the returned samples will provide numerous opportunities to study the characteristics of the Martian dynamo and its decay. Additionally, the inferred abundance of magnetic phases suggests that even mm-sized samples should be detectable by modern magnetometers. Samples that recorded a TRM will provide measurements of the paleointensity of the dynamo while samples that recorded a DRM could look for evidence of plate tectonics and true polar wander, in addition to creating a magnetostratigraphic record of the delta. Together, future and already cored samples promise to revolutionize our understanding of early Mars and the Martian dynamo.

References: [1] Weiss et al. (2008) *GRL,* 35, L23207. [2] Acuña et al. (1999), *Science*, *284*, 790-793. [3] Mittelholz et al. (2020) *Sci. Adv., 6*, eaba0513. [4] Dehant et al. (2007) *SSR, 129*. 279-300. [5] Farley et al. (2020) *SSR*, *216*, 142. [6] Farley et al. (2022) *Science*, *377*, eabo2196. [7] Allwood et al. (2020) *SSR,* 216. [8] Maurice et al. (2021) *SSR, 217. ;* Wiens et al. (2021) SSR, 2017 [9] Kizovski et al. (2022) *LPSC*. [10] Muxworthy and Williams (2006) *JGR,* 111. [11] Mandon et al. (2022) *JGR* [12] Wiens et al. (2022), *Sci. Adv.*, *8*, eabo3399. [13] Mandon et al. (2023) *LPSC LIV*. [14] Scheller et al. (2022) *Science*, *378*, 1105-1110. [15] Mandon et al. (2020) *Icarus*, *336*, 113436. [16] Dunlop and Özdemir (1997) *Cambridge University Press*. [17] Mangold et al. (2021) *Science, 374*, 711-717.

Incorporating the StraboSpot ecosystem into rock and paleomagnetic data collection practices

Nelson, E.M., Tikoff, B., Newman, J., Walker, J.D.

The StraboSpot ecosystem was developed to digitally collect, store, and share geologic field and laboratory data. The system is centered on three primary features: 1) StraboSpot mobile, an application designed for in-field collection of measurements, notes, images, samples, and other data; 2) StraboExperimental, which incorporates the results of experimental deformation; and 3) StraboMicro, which records thin section scale images, maps (e.g., optical, SEM, EBSD), and associated data. The key to all the StraboSpot systems is the ability to spatially nest observations over a variety of scales. Originally designed for structural geology field data, StraboSpot has been extended to incorporate petrology, sedimentology, and tephra volcanology workflows. Here, we explore possible avenues for future collaboration between the StraboSpot data system and MagIC. MagIC provides a central link for researchers to share and discover paleomagnetic data, however there are few tools designed for the collection of digital paleomagnetic data in the field. The benefits of integrating the StraboSpot field app into the MagIC hierarchy include: 1) increased findability of data through use of a cohesive vocabulary implemented during data collection; 2) increased efficiency by which paleomagnetic data is entered into the database; and 3) preservation of spatial information through hierarchical organization of images and data. Taking a community-based approach, we will design paleomagnetic modules within the StraboSpot field application that allow for seamless sharing of magnetic data between the two systems. These efforts would require us to incorporate the vocabulary, standards, and workflow utilized by the paleomagnetic community for fieldwork into the StraboSpot data system. Similar discussion could occur for other magnetic techniques that requires spatial information (e.g., Anisotropy of Magnetic Susceptibilities, Bulk Susceptibility). Overall, interoperability between the StraboSpot ecosystem and MagIC would increase the accessibility and findability of paleomagnetic data in the broader geologic community, fostering interdisciplinary research and adoption of paleomagnetic techniques.

New Paleomagnetic Record and $^{40}Ar/^{39}Ar$ Ages from Trindade Island, Brazil.

N.G. Pasqualon[1,2], J.F. Savian[2], E.F. Lima[2], W.P. de Oliveira[3], G.A. Hartmann[3], F.R. da Luz[2], R.I.F. Trindade[4], D. Miggins[5], E. B. Cahoon[5], A. Koppers[5], C.M.S. Scherer[2], L.M.M. Rossetti[6], A. Di Chiara[7]

[1]Department of Earth and Planetary Sciences, University of Hawaii at Manoa, Honolulu, HI, USA. [2]Instituto de Geociências, Universidade Federal do Rio Grande do Sul, Porto Alegre, RS, Brazil. [3]Instituto de Geociências, Universidade Estadual de Campinas, Campinas, SP, Brazil. [4]Instituto de Astronomia, Geofísica e Ciências Atmosféricas, Universidade de São Paulo, São Paulo, SP, Brazil. [5]College of Earth, Ocean, and Atmospheric Sciences, Oregon State University, Corvallis, OR, USA. [6]Instituto de Geociências, Universidade Federal do Mato Grosso, Cuiabá, MT, Brazil. [7] Instituto Nazionale di Geofisica e Vulcanologia, Rome, IT.

Keywords: South Atlantic Anomaly, Brunhes-Matuyama, Transitional Field.

Earth's magnetic field across the South Atlantic Ocean is characterized by anomalously low intensity values. The lowest field intensities are associated to the South Atlantic Anomaly (SAA), which has been investigated to provide a better understanding of Earth's core dynamics and the implications for core-mantle interactions (e.g., Hartmann and Pacca, 2009; Tarduno et al., 2015; Trindade et al., 2018; Shelby et al., 2020). Here, we present new paleomagnetic results of Trindade Island and $^{40}Ar/^{39}Ar$ ages for the volcanic and subvolcanic rocks of Trindade Island, which is a volcanic island located at 1.260 km from the Brazilian coast in the South Atlantic Ocean. The location of Trindade is ideal for investigating the geomagnetic field behavior and the SAA evolution on a scale from thousands to millions of years.

Trindade Island is composed of lava flows, intrusions, and pyroclastic rocks of strongly alkaline, SiO_2 undersaturated nature, and can be divided into five geological units (Almeida, 1961): Trindade Complex (TC), Desejado Sequence (DS), Morro Vermelho Formation (MV), Valado Formation (VA) and Paredão Volcano (PV) (Fig. 1). The two oldest units have well-constrained K/Ar ages from 3.9-1.5 Ma (Cordani, 1970, Pires et al., 2016). However, there is a gap in understanding the age relations between the three youngest units, which are thought to have occurred concomitantly or in a short time interval between them. Our study contributes to the acquisition of new paleodirectional data and improves the temporal resolution of radiometric data from Trindade Island.

Paleomagnetic data was acquired from 17 sampling sites, including phonolitic necks (7) and a melanephelinitic dyke (1) from Trindade Complex, and olivine-rich melanephelinitic aa flows from Morro Vermelho (4), Valado (3), and Paredão Volcano (2) formations. The Desejado Sequence was not sampled because of logistic issues. The magnetic mineralogy was investigated through thermomagnetic cycles, isothermal remanent magnetization (IRM) curves, hysteresis loops and first order reversal curves (FORC) diagrams and its results are described in detail by Pasqualon et al. (2020).

Alternating field (AF) and thermal (TH) demagnetization procedures were performed in a total

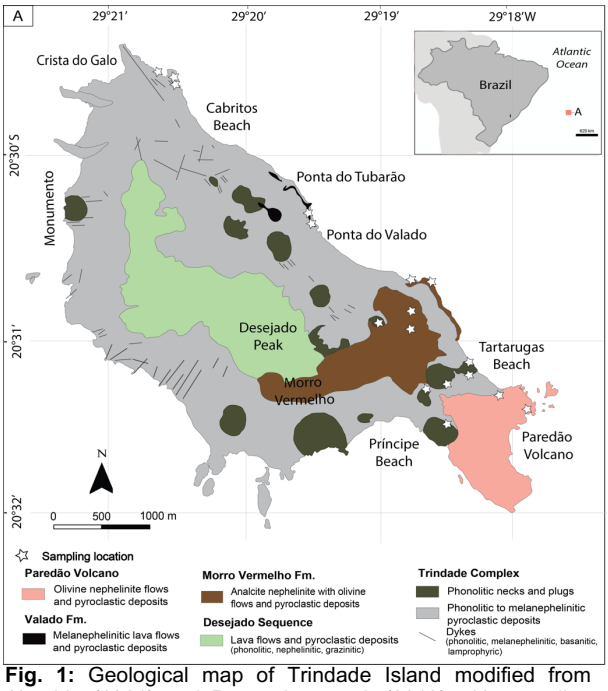

Fig. 1: Geological map of Trindade Island modified from Almeida (1961) and Pasqualon et al. (2019) with sampling locations indicated by stars.

of 504 oriented specimens using a JR6A spinner magnetometer and a 2G cryogenic magnetometer equipped with a RAPID system, at USPMag. Principal component analysis (PCA) was conducted through Remasoft 3.0 software. The lowest maximum angle deviation values (MAD < 10°) were accomplished when PCA was anchored to the origin and last point. Sites mean directions were calculated using at least 4 consecutive demagnetization steps (Fig. 2).

Six new high-precision $^{40}Ar/^{39}Ar$ ages were obtained for the youngest formations (MV, VA and PV) (Table 1) by incremental heating methods using the ARGUS-VI mass spectrometer. Groundmass samples were irradiated for 1 hour in the TRIGA CLICIT nuclear reactor at Oregon State University, along with the FCT sanidine flux monitor (Kuiper et al., 2008). Groundmass separates were prepared using standard procedures (Koppers, 2002). Besides sample VP-01C, these samples were also briefly leached in a mild (10%) Hydrofluoric Acid bath. Samples yield robust plateau ages with errors reported at 2 sigma.

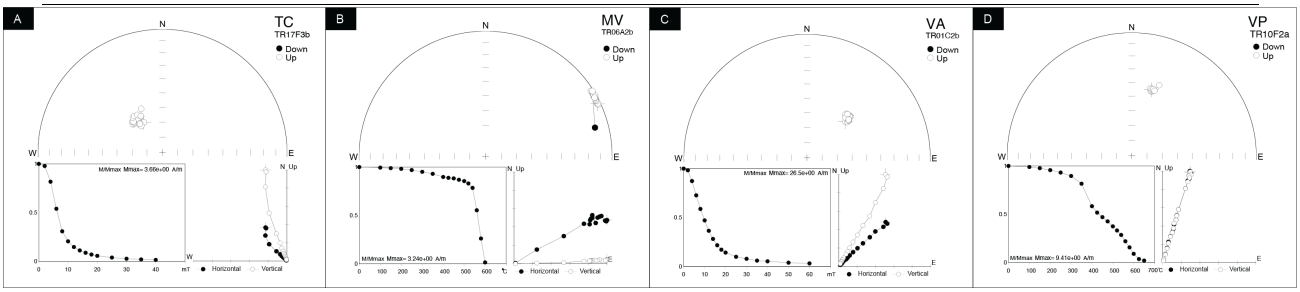

Fig. 2: Demagnetization diagrams, stereographic projections and magnetization intensity curves for sites of TC (A), MV (B), VA (C) and VP (D).

Sites from Trindade Complex (~2.9-2.8 Ma) were AF demagnetized between 30-40 mT (Fig.2A), associated with the presence of magnetite or low-Ti magnetite as main magnetic carrier. This unit presents a normal polarity and fits well within the Gauss normal polarity interval (Fig.3), with mean direction (n=7) of *D*= 247.04° and *I*= -48.17°. The Morro Vermelho (0.76-0.23 Ma) and Valado (0.48-0.08 Ma) sites were AF demagnetized around 35 mT (Fig.2C), displaying normal polarities with mean (n=4) *D*= 52.15° and *I*= -27.7°, and (n=3) D= 136.56° and I= -41.46°, respectively, coincident to the normal intervals within Matuyama and Brunhes Chrons (Fig.3).

Site TRGF-06 from Morro Vermelho Fm. (760.0 ± 78.4 ka) (Fig.2B) contains hematite and the best results were found by thermal treatments. This site is consistent with a transitional field between Brunhes and Matuyama (Fig.3), with *D*= 4° and *I*= -6.2°. Sites from the Paredão Volcano (0.22-0.06 Ma) also presented better THD results (Fig.2D), because of the presence of high-coercivity magnetic minerals. This formation displays normal polarity within the Brunhes Chron, with mean direction (n=2) of *D*= 207.65° and *I*= -52.25°.

Our new age data implies on a revised stratigraphy for the youngest units of Trindade Island, suggesting that Morro Vermelho volcanism started before Valado and Paredão Volcano. However, Valado overlaps Morro Vermelho volcanism for ~200 kys, while Paredão Volcano started at the very late stages of MV. The revised ages for Paredão volcano suggest the youngest Brazilian volcano last erupted at approximately 59.4±12 ka.

The interpretation and integration of a complete paleomagnetic and geochronologic dataset of Trindade Island volcanic and subvolcanic units provides the record of the geomagnetic field behavior over the past 3 Ma in the South Atlantic region, improving the understanding of the SAA longevity.

Table 1. Summary of groundmass $^{39}Ar/^{40}Ar$ ages for Trindade.

Sample	Sample Location	Age (ka)	Error (±2σ)	MS WD	no. steps
MV-N7 (HF)	MV (lower)	760.0	78.4	0.6	12.0
TR-06 (HF)	MV(upper)	231.5	76.2	0.9	14.0
TR-16 (HF)	VA (lower)	487.9	67.0	1.2	11.0
VA-04 (HF)	VA (upper)	77.7	125.1	0.6	8.0
VP-03B (HF)	PV (lower)	216.9	67.7	1.6	13.0
VP-01C	PV (upper)	59.4	12.0	1.6	12.0

Acknowledgements

The authors acknowledge the financial support of the CNPq - Project CNPq-442812/2015-9, the Graduate Program in Geosciences of UFRGS (PPGGEO), and Fapesp Project 19/22084-8 (Resp. V.A. Janasi).

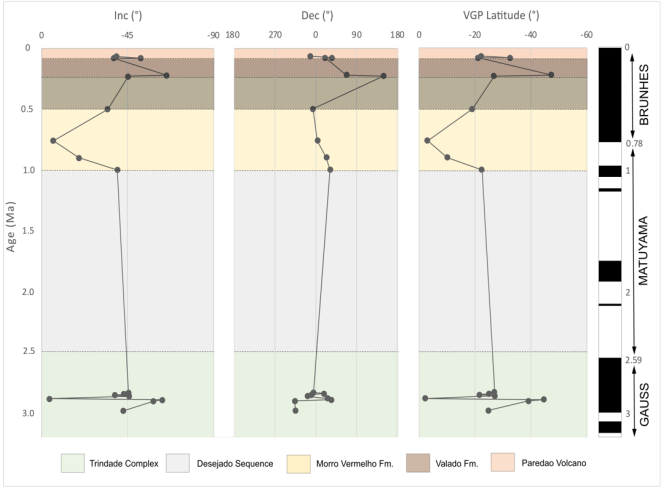

Fig. 3: Correlation of Inclination, Declination and VGP latitudes with the GPTS 2020 for Trindade Island units.

References

Almeida, F.F.M., 1961. Geologia e petrologia da Ilha da Trindade. 197f. Monografia XVIII, DGM/DNPM. Ministério das Minas e Energia, RJ.

Cordani, U.G., 1970. Idade do vulcanismo no Oceano Atlântico Sul. Bol. Inst. Geoc. Astron. USP. São Paulo, 1:9-75.

Gradstein F. M., Ogg J. G., Schmitz M., Ogg G., The geologic time scale 2012. Elsevier, 2012.

Hartmann, G. A., Pacca, I. G., 2009. Time evolution of the South Atlantic magnetic anomaly. An. Acad. Bras. Cienc., 81, 243–255.

Koppers, A. A. (2002). ArArCALC—software for 40Ar/39Ar age calculations. *Computers & Geosciences*, *28*(5), 605-619.

Kuiper, K. et al., 2008 Synchronizing rock clocks of history. Science, v. 320, pp.500–504.

Pasqualon, N. G., Lima, E. F., Scherer, C.M.S., Rossetti, L. M. M., Luz, F. R. 2019. Lithofacies association and stratigraphy of the Paredão Volcano, Trindade Island, Brazil. Journal of Volcanology and Geothermal Research, 380, 48-63.

Pasqualon, N.G., Savian, J.F., Lima, E.F., Luz, F.R., Moncinhatto, T.R. and Trindade, R.I., 2020. Emplacement dynamics of alkaline volcanic and subvolcanic rocks in Trindade Island, Brazil. Journal of Volcanology and Geothermal Research, 406, p.107078.

Pires, G.L.C., Bongiolo, E.M., Geraldes, M.C., Renac, C., Santos, A.C., Jourdan, F., Neumann, R., 2016. New 40Ar/39Ar ages and revised 40K/40Ar* data from nephelinitic–phonolitic volcanic successions of the Trindade Island (South Atlantic Ocean). J. Volcanol. Geotherm. Res. 327, 531–538.

Trindade et al., 2018. The future of the South Atlantic anomaly and implications for radiation damage in space. Natl. Acad. Sci. U.S.A., 115(52).

A lower reversal in the Picture Gorge Basalt: Implications for Columbia River Basalt Group Relations

A.F. Pivarunas[1], M.S. Avery[1], J.T. Hagstrum[1]

[1]U.S. Geological Survey, Geology Minerals Energy and Geophysics Science Center

The Picture Gorge Basalt (PGB) is a minor component of the Columbia River Basalt Group (CRBG) in eastern Oregon. It is the smallest continental flood basalt, yet it still encompasses an estimated 210,000 km^3 of lava. The hundreds of lava flows that comprise the CRBG are divided into the following major formations or eruptive phases: the Steens, Imnaha, Grande Ronde, Prineville, and Picture Gorge Basalts, with the Wanapum and Saddle Mountains Basalt eruptions subsequently taking place over an extended period. The Picture Gorge Basalt is smaller in volume and is considered coincident in time with the more voluminous Grande Ronde Basalt. Recent $^{40}Ar/^{39}Ar$ geochronologic work suggests an extended period of eruption for the PGB and has increased its mapped distribution.

Paleomagnetism is a useful tool for testing this extended emplacement paradigm, but there is no recent paleomagnetic work for the Picture Gorge Basalt. The magnetostratigraphy of its lavas at the type section is simple: lower flows are normal polarity, and then near the top of the flow sequence lavas transition to reverse polarity in the space of a few flows. This N-to-R sequence is typically considered coincident with the N1-R2 reversal in the Grande Ronde Basalt.

Our new work on the oldest lava flows in the Picture Gorge Basalt (PGB) below the type section reveals a lower reversal in multiple exposures. These PGB sites in eastern Oregon are located west of the town of Spray, near Girds Creek, and along the highway between Spray and Heppner. A reverse flow is found in both the Spray and Twickenham sections, and a transitional flow found in three sections allowing the more detailed Highway 207 section to be correlated with the type section in Picture Gorge.

These magnetostratigraphic results extend the known interval of PGB volcanism. Either PGB volcanism lasted throughout (CRBG) polarity chrons R1-N1-R2, or it began in R0 (coincident with the Steens Basalt) and took place during (CRBG) polarity chrons R0-N0-R1. Field relationships indicate that the former is more likely since (fluxgate) normal polarity PGB flows have been found interbedded with (fluxgate) normal polarity GRB flows in central Oregon at the Butte Creek section. This would be an unlikely occurrence in the latter scenario since GRB

was not erupting in N0 time. Thus, more work is needed to fully understand the PGB and GRB relationships. Our work partially vindicates the suggestion of an extended interval of PGB volcanism; however, we find that the PGB is unlikely to have lasted through the entire main phase of the CRBG without unrecognized hiatuses.

Rock magnetic characterization of the San Juan de Otates Ultramafic-Mafic Complex, Mexico

Ramirez-Garcia, S., B.

The San Juan de Otates Ultramafic-mafic Complex (SJO-UMM) comprises serpentinized dunites, partially serpentinized wehrlites and olivine-clinopyroxenites, and gabbro. Oxide minerals within the ultramafic lithologies are fine to very fine magnetite (200-50 μm), very fine ferritchromite (100-25 μm), secondary maghemite (50 μm) and, occasionally, some sulfurs (Fig.1a). Magnetite and Fe-chromite growing textures are associated with pseudomorphic serpentinization textures. The most prominent presence of magnetite tends to be related to coarse veins surrounding the serpentine. Magnetic remanence of ultramafic rocks ranges from 1.39 to 240 A/m, and susceptibility is up to 0.22 SI. The magnetite content decreases as the amount of clinopyroxene increases. Thus, the serpentinized dunites have up to 40% magnetic mineral volume, while the olivine-clinopyroxenites have just 3% rock volume. Magnetic hysteresis and FORC diagrams suggest that magnetic particles in ultramafic rocks have magnetic domain sizes in the vortex state. Serpentinized dunites have magnetic grain sizes greater than three μm, as well as wehrlites which have less magnetic coercivity. Olivine-clinopyroxenites have a mixture of magnetic particle sizes from 0.2 μm to <3 μm. The degree of serpentinization of serpentinized dunites is greater than 90%. Wehrlites range between 60-90%, and olivine-clinopyroxenites exhibit serpentinization degrees between 20% and 80%. The serpentinization percentage does not display a statistical relationship between the magnetite content and the NRM or the magnetic susceptibility. Our findings indicate that the magnetic properties of the serpentinized rocks from the SJOUMM are not determined by the serpentinization degree (Fig. 1b). Instead, the magnetic characterization suggests that serpentinization was a complex process. Evidence from demagnetization analyses and the occurrence of magnetite, Fe-chromite, and Cr-magnetite indicate that the serpentinization degree occurred between 200 °C and 350 °C. Previous tectonic models for the origin and evolution of the San Juan de Otates Ultramafic-mafic Complex allow correlating the serpentinization temperatures probably during the exhumation of the complex at the time of the Arperos basin closure (ca. 100 Ma).

The differences in the magnetite content, the magnetic properties, and the serpentinization conditions that we found in our study support the proposed evolutionary model for the SJOUMM as a Ural-Alaskan type arc by fractional crystallization. This study found that the susceptibility and the NRM do not behave similarly to the serpentinized ultramafic rocks from other settings, such as MORs. Additionally, we advocate for studying the magnetic properties of ultramafic rocks to identify their origin. Therefore, the magnetic characterization of the San Juan de Otates Ultramafic-mafic Complex provides insight into the poorly studied Ural-Alaskan complexes.

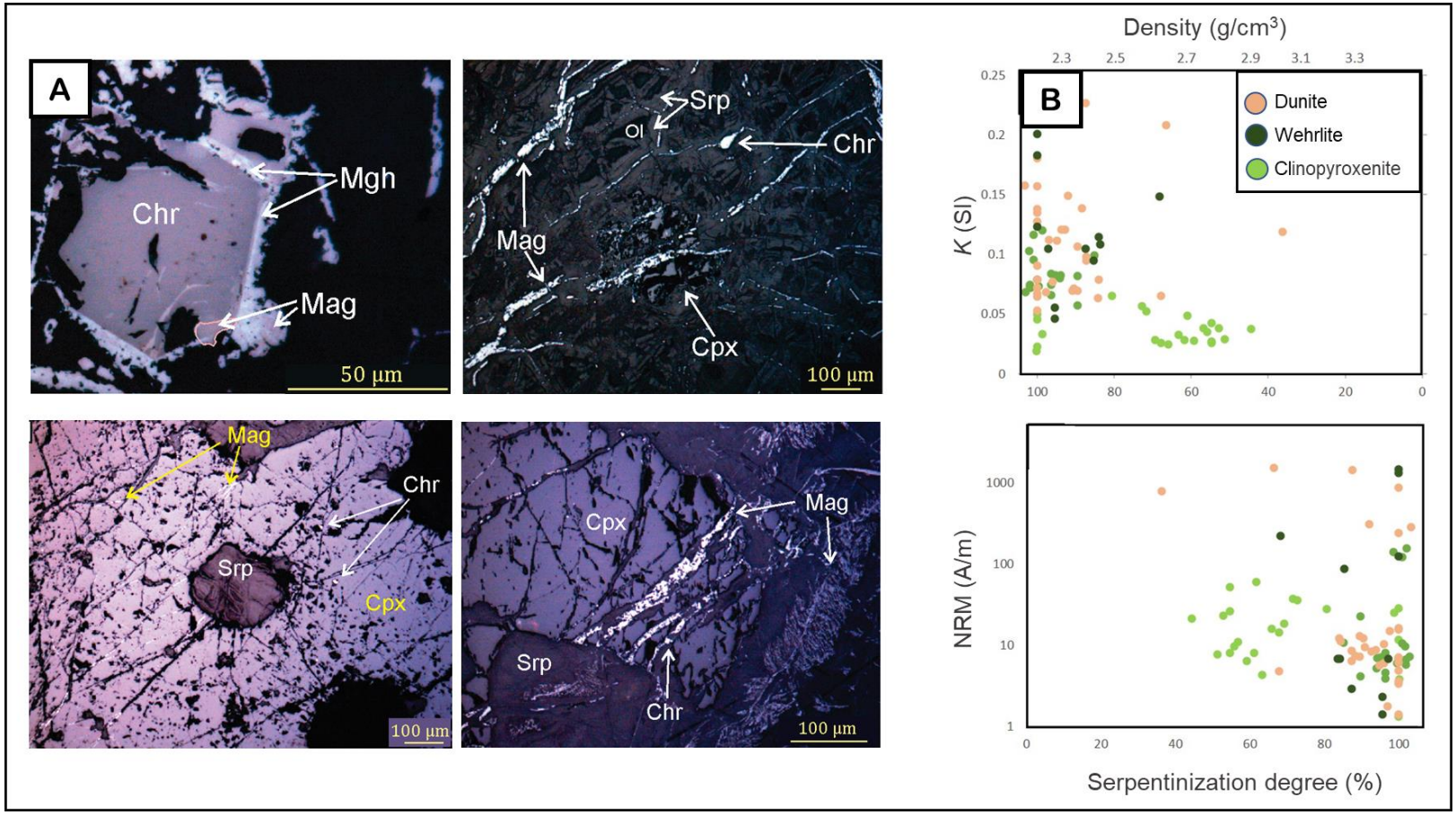

Figure 1. A) Micro-textures of magnetite within ultramafic rocks. B) Relationship between magnetic parameters (NRM and K) and the serpentinization degree.

What's signal and what's noise in sediment paleomagnetic secular variation (PSV) records? Investigating five well-dated 'ultra-high' resolution records from the Northern North Atlantic.

Brendan Reilly[1] and Joseph Stoner[2]

[1]Lamont-Doherty Earth Observatory, Columbia University, Palisades, NY, USA

[2]College of Earth, Ocean and Atmospheric Sciences, Oregon State University, Corvallis, OR, USA

We investigate the amplitude and frequencies of geomagnetic change in the Northern North Atlantic (66-68^{o} N) using 5 'ultra-high' resolution sediment cores deposited at accumulation rates in excess of 1m/kyr that span the last 15 kyr. The ages of these cores are constrained by 71 radiocarbon dates with reservoir ages determined through tephra correlation to terrestrial archives. Our study aims to address many of the uncertainties that are common in sedimentary paleomagnetic studies, including signal attenuation in low to moderate resolution archives and difficultly to demonstrate reproducibility in higher resolution archives. The 'ultra-high' accumulation rates of our cores reduce 'lock-in' and smoothing uncertainties associated with magnetic acquisition processes. Abundant radiocarbon dates provide tests of signal reproducibility at sub-millennial timescales. We use an objective dynamic time warping (DTW) algorithm to align each core's inclination and declination signal simultaneously on a synthetic regional depth scale. Comparison of radiocarbon constraints migrated to this synthetic regional depth scale show excellent stratigraphic agreement, providing an average of 1 date every 210 years. The result is a 15 kyr stack, GREENICE15, that validates prior results, but provides stronger geochronological constraint, demonstrates a reproducible PSV signal and amplitude, and extends through the abrupt Bølling–Allerød and Younger Dryas climate transitions of the latest Pleistocene. Results are consistent with what is expected from spherical harmonic models and previously published data from Northern Europe, but shows higher amplitude of directional change—particularly on sub-millennial timescales. We discuss the timescales and amplitude of directional geomagnetic change in the Northern North Atlantic with respect to regional sedimentary records. Additionally, our stack can be used as a new tuning target for often difficult to date Pleistocene-Holocene transition records and has a transparent chronology that can be updated as our understanding of time variations in marine reservoir age improves.

Preliminary paleomagnetic results from the Reykjanes Ridge, North Atlantic Ocean (IODP Expeditions 384 and 395C)

Sara Satolli[1], Anita Di Chiara[2], Sarah Friedman[3], and Expedition 395 Science Party[4]
[1] Department of Engineering and Geology, University of Chieti-Pescara, Italy (s.satolli@unich.it)
[2] INGV, Rome, Italy (anita.dichiara@ingv.it)
[3] Department of Geology and Geography, Georgia Southern University, GA, USA (sfriedman@georgiasouthern.edu)
[4]expedition_395_participants@iodp.tamu.edu

The International Ocean Discovery Program (IODP) Expeditions 384 and 395C targeted the Reykjanes Ridge, located in the North Atlantic Ocean, southwest of Iceland, and will be complemented by Expedition 395 during summer 2023. The Reykjanes Ridge is characterized by a series of V-shaped ridges (VSRs) and troughs (VSTs), the formation of which has yet to be understood. The shared objectives of these three expeditions are: (1) to investigate temporal variations in ocean crust generation at the Reykjanes Ridge, (2) to analyze sedimentation rates and contourites, and (3) to analyze the alteration of oceanic crust. For the time being, five sites were drilled along a transect eastwards of the modern Mid-Atlantic Ridge (between 20-30°W) at a latitude of ~60°N, to investigate VST/VSR formation.
In this preliminary study, we analyze shipboard data from the five drilled sites, and preliminary data from discrete samples collected in sediments and basalts during the post-cruise research. Sediment shipboard data were processed removing edge effects and isolating the magnetization through the principal component analysis. Discrete samples are being analyzed at CIMaN-ALP (Peveragno) and INGV (Rome) Laboratories of paleomagnetism through anisotropy of magnetic susceptibility (AMS) and alternating field or temperature stepwise demagnetization of natural remanent magnetization (NRM). Basalts samples are also analyzed using hysteresis loops and FORC diagrams, and susceptibility vs temperature curves.
The sedimentary sequences, coupled with biostratigraphic data, allowed defining an age model for the five drilled sites, and reconstruct the sedimentary rate variations along the studied transect linked to the ridge evolution. The sedimentary sequences also show a record of geomagnetic instabilities during the Brunhes (0-0.778 Ma). Constraining the chronology of these geomagnetic instabilities is fundamental to understanding Earth's dynamo processes and their surface expressions. Moreover, a detailed geomagnetic instability time scale refines its applicability as an accurate correlation and dating tool (magnetostratigraphy) for sedimentary and volcanic sequences and it is fundamental to understanding several aspects of past climate.
Basalt samples from four sites, two from VSRs and two from VSTs were investigated to define the differences between ridges and troughs, and correlations with the degree of alteration observed in the basalts. Preliminary results shows that basalts from VSTs are generally characterized by higher susceptibility values. The magnetic fabric, tentatively used as a proxy for basalt alteration, show a mixed behavior (well defined or dispersed) independently from the structural position.

A new view on the magnetic history of the Moon

J.A. Tarduno[1,2,3], T. Zhou[1], R.D. Cottrell[1]

[1]Department of Earth & Environmental Science, Univ. Rochester, Rochester, NY 14627
[2]Department of Physics & Astronomy, Univ. Rochester, Rochester, NY 14627,
[3]Laboratory for Laser Energetics, Univ. Rochester, Rochester, NY 14623

Inspired by the studies of Apollo samples by Kristin Lawrence and colleagues (1), recent single crystal paleointensity investigations at the University of Rochester provide evidence for the lack of a lunar dynamo at and after 3.9 Ga, whereas studies of young lunar glass at the University of Rochester provide evidence that impacts can impart magnetizations (2). Together, these data provide the basis for a new view whereby the Moon lacks a long-lived magnetic field of internal origin (2). This new understanding resolves the conundrums posed by prior interpretations calling for a past long-lived lunar dynamo, producing a surface field at times as strong or stronger than Earth's field (3) and spanning some 2 billion years (4). These long-lived dynamo interpretations have been paradoxical because of a lack of energy to produce such a sustained field (5), and because of a lack of time-correlative strong, long wavelength lunar magnetic crustal anomalies (6). The absence of a long-lived lunar paleomagnetosphere is important for future scientific exploration on the Moon. With a lunar magnetosphere, Earth's early atmosphere can be transported to the paleo-lunar surface and preserved in buried lunar soils (2,7). This transfer is further aided by the intensity of early solar winds (8).

Here, we address some remaining unknowns about the magnetic history of the Moon. These include the full understanding of processes responsible for high field values reported from nonthermal paleointensity measurements from some Apollo rocks. These values have recently been used to support a model of a transient dynamo (9), but there remains a mismatch with power requirements. In addition, a thermally driven dynamo is feasible for the first several hundred million years of lunar history, and this could play a role in forming weak magnetic anomalies recorded in the south polar region of the Moon (10), and possibly in larger areas (but not all) of the deep lunar crust (6). The age of such a potential early dynamo, however, is unknown. We investigate the nature of high field values from prior nonthermal paleointensity analyses through a study of paired single crystal paleointensity (SCP) and whole rock paleointensity studies of ~3.8 Ga Apollo mare basalts. We study the possibility of an early dynamo through SCP analyses of a 4.3 Ga Apollo anorthosite. Specifically, the samples investigated are Apollo 17 70035, a high-Ti mare basalt with a mean age derived from multiple $^{40}Ar/^{39}Ar$ and Rb-Sr geochronological analyses (11) and updated decay constants of ~3.8 Ga, and Apollo 16 60025, a ferroan anorthosite with an age of 4360 ± 3 Ma based on multiple isotopic systems (12).

We separate single silicate crystals (feldspar) using non-magnetic tools for SCP analyses (13). Silicate crystals analyzed in this investigation are approximately 0.5 mm in size. Bulk rock samples analyzed from Apollo 70035 are approximate 3 mm in size. We use the ultra-sensitive WSGI 3-component DC SQUID magnetometer in the University of Rochester's magnetically shielded room (ambient field < 200 nT) and CO_2 laser heating techniques (14) which afford heating times more than an order of magnitude shorter than standard paleomagnetic ovens. Samples are heated and cooled rapidly in air; a controlled (reducing) atmosphere is not used because this can promote further reduction and the formation of new magnetic particles (2,15). We use non-magnetic materials, documented in multiple laboratories (16), to mount crystals. We investigate magnetic mineralogy using the Univ. Rochester Zeiss Auriga scanning electron microscope (SEM) with an energy dispersive x-ray analysis (EDAX).

We find that the natural remanent magnetizations (NRM) of 70035 feldspar crystals are extremely weak, suggesting that their magnetic minerals cooled in the absence of a magnetic field. Moreover, we find a magnetization indistinguishable from zero after heating to 590 °C, a temperature where considerable magnetization of lunar magnetic carriers should be unblocked. Given this null magnetization state, the

standard Thellier paleointensity approach is meaningless. Instead, we assess whether the crystals can record a magnetic field in accordance with magnetization theory (17) by the following procedure (2). First, we impart a partial thermoremanent magnetization (pTRM) at 590 ºC in the presence of a 20 μT field. The sample is then demagnetized by heating to 590 ºC, and the magnetization is? assessed to determine whether it returned to the null magnetization state. Next, a pTRM is imparted in a 40 μT field. The magnetizations of the two-field strength pTRMs allow a determination of the recording efficiency (2). We find the 70035 feldspars have high efficiencies and can record dynamo fields, but instead they record zero magnetization levels. As a final check of the magnetization recording, we conduct SEM and EDS analyses on the exact crystals used for SCP measurements. These analyses confirm that the crystals contain Fe-Ti magnetic carriers with single domain-like (SD) characteristics. Next, we analyze a bulk sample by nonthermal methods to compare with prior data. Our sample shows an irregular demagnetization pattern, but with a distinct component isolated up to ~50 mT. We use the REM' nonthermal method which yielded nominal paleointensity values between 10 and 20 μT.

We find that the NRM of feldspars from Apollo 60025 are extremely weak, consistent with null magnetizations. We check the recording fidelity by applying pTRMs at 20 and 40 μT; these yield magnetizations indicating that the crystals could record ambient magnetic fields had they been present, but they do not. SEM and EDS analyses demonstrate Fe-Ti magnetic particles having sizes and shapes indicating SD magnetic recording properties.

Our new results from ~3.8 Ga high-Ti basalt 70035 shed light on both the origin of Earth-like fields recorded by Apollo samples (3) and a potential transient dynamo (9). The single crystals have magnetic particles with ideal magnetic properties and recording efficiencies and record null ambient fields, whereas the bulk rocks, known to contain nonideal magnetic particles, yield relatively strong fields using nonthermal techniques. These data are consistent with there being no field during the cooling of high-Ti basalt 70035 at ~3.8 Ga, but that sometime later the bulk sample was affected by a shock remanent magnetization (SRM) with the ambient field supplied by an impact plasma (2). A similar finding results from a comparison of SCP results for the 3.95 Ga Apollo 14 low-Ti/high-Al basalt 14053 (18), which yielded a null magnetization (5), and bulk samples which yield 20 μT magnetic field intensities using the nonthermal REM' method (19). We note that if the shock remanent magnetization is less efficient than a thermal remanent magnetization, the field values estimated using the REM' method could be underestimated by as much as a factor of 3 (20). However, this is still well within the range of fields produced by impact charge-separation (21-23). Such an underestimate must be weighed against the potential for false high paleointensity readings with nonthermal techniques. Notwithstanding the uncertainties inherent to nonthermal methods, shock magnetizations with ambient fields supplied by impact plasmas can explain the enigmatic nominal high paleointensities (3) derived from other Apollo samples. Because an episodic dynamo relies on these values (9), we conclude there is no reliable evidence from Apollo samples supporting its existence. Our data further extend back in time the period of lunar history lacking a strong sustained dynamo to 4.3 Ga. Hence, our new data are compatible with the potential presence of a core dynamo in the Moon only during its first 200 million years.

References: (1) Lawrence, K. et al., *Phys. Earth Planet. Inter. 168*, 71–87 (2008). (2) Tarduno, J. A. et al. (2021) *Sci. Adv., 7* eabi7647. (3) Fuller, M., and Cisowski, S. M. (1987) *Geomag., 2*, 307–455. (4) Tikoo, S. M. et al., (2017) *Sci. Adv., 3,* e1700207. (5) Evans, A. J. et al. (2018) *GRL 45*, 98–107. (6) Wieczorek, M. A. (2018) *JGR 123*, 291–316. (7) Fagents, S. A., et al. (2010) *Icarus 207*, 595–604. (8) Tarduno et al. (2011) *PEPI 233,* 68-87. (9) Evans, A. J. and Tikoo, S. M. (2022) *Nat. Astron., 6*, 325-330. (10) Hood, L. L. et al. (2022) *GRL, 49,* e2022GL100557. (11) Paces, J. B. et al. (1991) *GCA, 55*, 2025-2043. (12) Borg, L. E. et al. (2011) *Nature*, *477*, 70–72. (13) Tarduno, J. A. et al. (2006) *Rev. Geophys., 44,* RG1002. (14) Tarduno, J. A. et al. (2007) *Nature*, *446*, 657-660. (15) Tarduno, J. A. et al. (2022), *LPSC 53rd*, 2566. (16) Tarduno, J. A. et al. (2020) *PNAS, 117*, 2309-2318. (17) Dunlop D. J. & Özdemir Ö. (1997) Cambridge Univ. Press. (18) Snape, J. F. et al. (2019) *GCA, 266*, 29-53. (19) Cournede, C. et al. (2012) *EPSL* 331-332, 31-41. (20) Gattacceca, J. et al. (2010) *EPSL, 299*, 42-53. (21) Crawford, D. A. and Schultz, P. H. (1988) *Nature 336*, 50–52. (22) Bruck Syal, M. and Schultz, P. H., (2015) *Icarus 257*, 194–206. (23) Crawford, D. A. (2020) *Int. J. Impact Eng., 137*, 103464.

Vector unmixing of multicomponent palaeomagnetic data

Justin A.D. Tonti-Filippini and Stuart A. Gilder

Department for Earth and Environmental Sciences, Ludwig Maximilian University of Munich, D-80333 Munich, Germany. E-mail: j.tonti@lmu.de

Abstract

Palaeomagnetic investigations often encounter multiple magnetization components, where secondary processes have obscured, partially overprinted or completely replaced the original (primary) remanent magnetization. Identification and separation of primary and secondary magnetizations are generally carried out with principal component analysis of stepwise demagnetization data. However, rocks may contain multiple generations of magnetic minerals with overlapping unblocking ranges that complicate the discrimination of components when applying best-fitting line procedures. Developing a method to differentiate and quantify contributions of overlapping magnetic components using directional data is therefore highly desirable. This paper presents a method to unmix stepwise demagnetization data using an inverse modelling approach. We show that the method is capable of accurately resolving two or three magnetic components with overlapping or superimposed unblocking spectra as well as quantifying absolute component contributions. The method depends on accurate identification and selection of end-member components prior to analysis; in doing so, the method can help palaeomagnetists understand how magnetization components combine to explain their data. We show that the dilution of one component by more than ca. 25 per cent from another component can result in linear demagnetization curves that decay to the origin on orthogonal plots, but whose best-fitting direction can significantly deviate from both end-members. The efficacy of the method is demonstrated through examples of demagnetization data from hematite and/or magnetite-bearing sandstones from China. This method can be broadly applied to all multicomponent magnetization problems in palaeomagnetism.

Lithology Dependence of Magnetic Behaviour and Fidelity

Alexander Tully, Greig Paterson

University of Liverpool

Currently our best predictions of future variations in Earth's magnetic field are too short to meet the needs of long term investments, such as for satellites and ground based infrastructure. From current research frontiers such as understanding the evolution of the deep Earth and the physics of extreme geomagnetic features, implications for the predictability can be made. However, this is impeded by uncertainty in the reliability of palaeointensity data.

We are developing state of the art palaeointensity stochastic models in order to approach this challenge. These models will be able to simulate experiments and provide a new a big data methodology to assess the uncertainty of the result. In order to ground truth these models vast amounts of data are needed as inputs, far more than can be acquired individually, as such open access data, e.g. the MagIC database, is vital to this data-driven endeavour.

We present new insights in the reliability of differing lithologies for palaeointensities through complied hysteresis and demagnetisation datasets, obtained through data-mining the MagIC database and beyond, from which a better understanding of the impact they have on experimental results can be gathered.

Hong Yang
hyang777@stanford.edu

Can we use field dependence of susceptibility to identify the magnetic mineralogy of submarine basalts?

Hong Yang[1], Sonia M. Tikoo[1], Dario Bilardello[2], Peat Solheid[2] and the Expedition 391 Scientists*
[1] Department of Geophysics, Stanford University, CA 94305, USA
[2] Institute for Rock Magnetism, University of Minnesota, MN 55455, USA
* https://iodp.tamu.edu/scienceops/precruise/walvis/participants.html

Oceanic basalts, covering nearly 2/3 of Earth's surface, are a database of Earth's magnetic field records. To decipher this information, different paleomagnetic methods are applied depending on individual sample's rock magnetic properties. Because of the complex magnetic mineralogy of submarine basalts[1–3], it may be difficult to figure out whether alternating field (AF) or thermal demagnetization methods are better suited for each sample a priori. Due to the (magnetically) destructive nature of AF or thermal treatment, it is desirable to have a fast, non-destructive pre-screening method to decide which demagnetization method would be most appropriate (Fig. 1). Such a method may be particularly helpful in scientific ocean drilling expeditions where recovered material is limited. The field dependence of magnetic susceptibility (MS) (also referred to as amplitude dependence) can be measured with an AGICO Kappabridge susceptibility meter in less than 5 minutes. Herein, we present an initial survey of whether measuring field dependence of magnetic susceptibility may be used as a facile way to pre-screen samples, for choosing the most suitable demagnetization method for extracting magnetic field records from oceanic basalts.

We test this method on oceanic island basalts collected from the International Ocean Discovery Program (IODP) Expedition 391[4]. These basalts were sampled from the Walvis Ridge (Tristan-Gough) hotspot tracks in the southern Atlantic from four boreholes (U1575A, U1576B, U1577A, U1578A) with ages of ~100 Ma, ~80 Ma, ~84 Ma, and ~63 Ma respectively[5]. Variations in depositional styles (massive lava flows vs. pillow lavas), degree of weathering, and cooling rates provide a rich variety of magnetic mineralogies spanning the ulvöspinel-magnetite and ilmenite-hematite solid solutions. Using a Kappabridge MFK-2A susceptibility meter at the Stanford Paleomagnetism Lab, we first screened basalt samples using field strengths ranging from 1 A/m to 700 A/m. After identifying representative samples with low and high field dependence, we further characterized those samples' rock magnetic carriers and domain states using measurements of hysteresis loops, backfield remanence curves, First-Order Reversal Curve (FORC) diagrams, and low-temperature AC susceptibility measurements at the Institute for Rock Magnetism.

We found field-dependent behavior correlates well with the domain state of the sample (Fig.2). Samples exhibiting pseudo-single-domain-like behavior exhibit higher field dependence while single domain (SD) samples are field independent as expected. This is because for titanomagnetites, field-dependent behavior arises from low-field hysteresis of domain wall movement[6,7]. Therefore, a basalt sample with high field dependence indicates titanomagnetite composition in a domain state larger than SD. High field dependence thus imply the freshness of basalts as alteration may reduce the grain sizes of titanomagnetite or produce fine-grained maghemite in the samples. Therefore, field-dependence of MS can possibly help locate layers having undergone low degree of alteration that may be better-suited for paleointensity studies. Excluding stoichiometric magnetite compositions, if a sample possesses low to null field dependence, significant alteration is likely. Further analysis to correlate the FORC and low-temperature AC susceptibility data with field dependence is ongoing and will be presented at the workshop.

Hong Yang
hyang777@stanford.edu

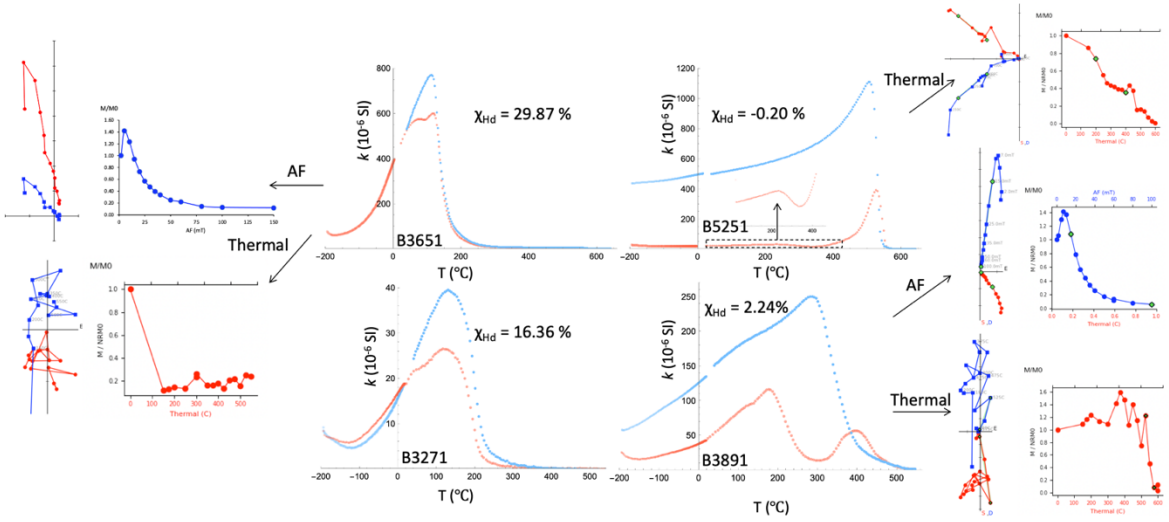

Figure 1. Representative thermomagnetic curves of basalts with different field dependence of MS, as well as their demagnetization behaviors. $\chi_{Hd} = (\chi_{300\ A/m} - \chi_{30\ A/m})/\chi_{30\ A/m}$. B5251 (U1576A, 381.27 m) is from a sheet flow, and other 3 samples are from massive lava flows. Samples (B3651 (U1585A, 252.26 m) and B3271 (U1578A, 218.55 m)) with high field dependence appear to show more reversible *k*-T curves. These samples also have low curie temperatures and AF demagnetization would be more suitable. Samples with low field dependence (B3891 (U1578A, 246.94 m)) have no clear preference for AF or thermal treatment based on current dataset.

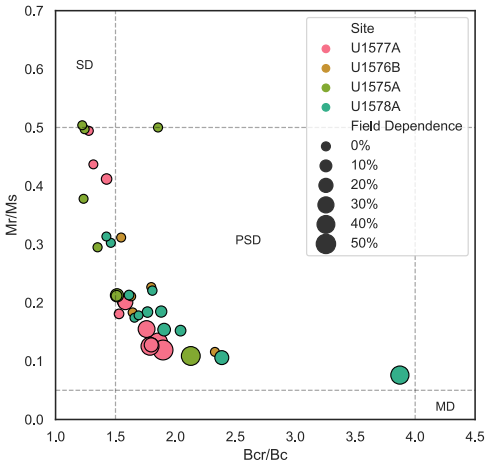

Figure 2. Day-plot of basalt samples with field dependence represented in dot size. Field dependence $\chi_{Hd} = (\chi_{300\ A/m} - \chi_{30\ A/m})/\chi_{30\ A/m}$. The basalt samples trend along the Day plot SD-MD mixing lines and samples with high field dependence are located closer to the MD region. They are also characterized by reversible *k*-T curves and low Curie temperature (Fig. 1).

Acknowledgments
We greatly thank Maxwell Brown for all the assistance in arranging the visit and the data collection at IRM.

References

[1] Zhou W, Van der Voo R, Peacor D R, Zhang Y 2000 *Earth Planet. Sci. Lett.* **179** 9
[2] Özdemir Ö 1987 *Phys. Earth Planet. Inter.* **46** 184
[3] Furuta T 1993 *Geophys. J. Int.* **113** 95
[4] Sager W, Hoernle K, Petronotis K 2020
[5] Expedition 391 Scientists, Sager W, Hoernle K, Höfig T W 2022
Expedition 391 Preliminary Report: Walvis Ridge Hotspot (International Ocean Discovery Program)
[6] Jackson M, Moskowitz B, Rosenbaum J, Kissel C 1998 *Earth Planet. Sci. Lett.* **157** 129
[7] Bilardello D 2023 *IRM Q.* **32-4**